

*Book by Nova Publishers*  
*“Moon: Geological Characteristics, Physical Characteristics and Exploration”*

**Chapter**  
**“Probing Gravitational Physics with Lunar Laser Ranging”**

Authors

Caterina Lops

Istituto Nazionale di Fisica Nucleare – Laboratori Nazionali di Frascati (INFN - LNF), Via Enrico Fermi 40, 00044 Frascati, Italy and University of Rome “Roma Tre”, Via della Vasca Navale 84, 00146 Rome, Italy

Manuele Martini

Istituto Nazionale di Fisica Nucleare – Laboratori Nazionali di Frascati (INFN - LNF), Via Enrico Fermi 40, 00044 Frascati, Italy

Co-authors

S. Dell’Agnello

Istituto Nazionale di Fisica Nucleare – Laboratori Nazionali di Frascati (INFN - LNF), Via Enrico Fermi 40, 00044 Frascati, Italy

D.G. Currie

Department of Physics, University of Maryland, College Park, Maryland 20742, USA

G.O. Delle Monache

Istituto Nazionale di Fisica Nucleare – Laboratori Nazionali di Frascati (INFN - LNF), Via Enrico Fermi 40, 00044 Frascati, Italy

C. Cantone

Istituto Nazionale di Fisica Nucleare – Laboratori Nazionali di Frascati (INFN - LNF), Via Enrico Fermi 40, 00044 Frascati, Italy

M. Garattini

Istituto Nazionale di Fisica Nucleare – Laboratori Nazionali di Frascati (INFN - LNF), Via Enrico Fermi 40, 00044 Frascati, Italy

A. Boni

Istituto Nazionale di Fisica Nucleare – Laboratori Nazionali di Frascati (INFN - LNF), Via Enrico Fermi 40, 00044 Frascati, Italy

S. Berardi

Istituto Nazionale di Fisica Nucleare – Laboratori Nazionali di Frascati (INFN - LNF), Via Enrico Fermi 40, 00044 Frascati, Italy

M. Maiello

Istituto Nazionale di Fisica Nucleare – Laboratori Nazionali di Frascati (INFN - LNF), Via Enrico Fermi 40, 00044 Frascati, Italy

L. Porcelli

Istituto Nazionale di Fisica Nucleare – Laboratori Nazionali di Frascati (INFN - LNF), Via Enrico Fermi 40, 00044 Frascati, Italy

G. Patrizi

Istituto Nazionale di Fisica Nucleare – Laboratori Nazionali di Frascati (INFN - LNF), Via Enrico Fermi 40, 00044 Frascati, Italy

N. Intaglietta

Istituto Nazionale di Fisica Nucleare – Laboratori Nazionali di Frascati (INFN - LNF), Via Enrico Fermi 40, 00044 Frascati, Italy

R. March

Istituto Nazionale di Fisica Nucleare – Laboratori Nazionali di Frascati (INFN - LNF), Via Enrico Fermi 40, 00044 Frascati, Italy and Istituto per le Applicazioni del Calcolo, CNR, Via dei Taurini 19, 00185 Rome, Italy

G. Bellettini

Dipartimento di Matematica, University of Rome “Tor Vergata”, Via della Ricerca Scientifica 1, 00133 Rome, Italy, and Istituto Nazionale di Fisica Nucleare – Laboratori Nazionali di Frascati (INFN - LNF), Via Enrico Fermi 40, 00044 Frascati, Italy

R. Tauraso

Dipartimento di Matematica, University of Rome “Tor Vergata”, Via della Ricerca Scientifica 1, 00133 Rome, Italy, and Istituto Nazionale di Fisica Nucleare – Laboratori Nazionali di Frascati (INFN - LNF), Via Enrico Fermi 40, 00044 Frascati, Italy

G. Bianco

Agenzia Spaziale Italiana (ASI), Centro di Geodesia Spaziale 'Giuseppe Colombo', Località Terlecchia 75100 Matera (MT), Italy

T.W. Murphy

Physics Department, University of California, San Diego, CASS-0424, 9500 Gilman Dr., La Jolla, CA 92093, USA

J.B.R. Battat

Center for Astrophysics (CfA), Harvard University, Cambridge, MA 02138 and Department of Physics, Massachusetts Institute of Technology, Cambridge, MA

J.F. Chandler

Center for Astrophysics (CfA), Harvard University, Cambridge, MA 02138

Duncan McElfresh

University of Colorado of Mines 1500 Illinois St Golden, CO 80401

M. Tibuzzi

Istituto Nazionale di Fisica Nucleare – Laboratori Nazionali di Frascati (INFN - LNF), Via Enrico Fermi 40, 00044 Frascati, Italy

C. Graziosi

Istituto Nazionale di Fisica Nucleare – Laboratori Nazionali di Frascati (INFN - LNF), Via Enrico Fermi 40, 00044 Frascati, Italy

## ABSTRACT

Lunar Laser Ranging (LLR) provides precise, metrologically absolute positioning measurements in the gravitational laboratory of the Sun - Earth - Moon System with a space segment based on cost-effective, passive, maintenance-free payloads. This technique consists in a time of flight (ToF) measurement of short laser pulses fired by stations of the International Laser Ranging Service (ILRS) on Earth to payloads of Cube Corner Retroreflectors (CCRs) on the Moon, which are (retro)reflected back to the stations. LLR and SLR (Satellite Laser Ranging) are absolute measurements because they are referred to the International Terrestrial/Celestial Reference System (ITRS/ICRS). As a matter of fact, the laser ranging geodesy technique is used to define the geocenter (Earth center of mass) and the scale, that is, origin and unit length of the ITRS/ICRS, respectively.

The LLR discipline was initiated in the late 1960's by the University of Maryland (UMD), Principal Investigator (PI) of the CCR array deployed on the Moon by the Apollo 11, 14 and 15 missions. Thanks to the measurements of lunar orbit with an accuracy of a few centimeters (based on the Apollo and one Russian Lunokhod CCR arrays) several predictions of General Relativity have been tested, including: the Weak and Strong Equivalence Principle, the geodetic precession, the parameterized post-Newtonian parameters  $\gamma$  and  $\beta$ , the constancy of the gravitational constant  $G$  and a non-newtonian of the Yukawa form.

A US-Italy collaboration of UMD and the Istituto Nazionale di Fisica Nucleare - Laboratori Nazionali di Frascati (INFN-LNF) started an effort to improve both the LLR instrumentation and modeling in the framework of the LLRRA21 project (Lunar Laser Ranging Retroreflector Array for the 21<sup>st</sup> century) for the Lunar Sortie Science Opportunities (LSSO) NASA Program<sup>1</sup> and of MoonLIGHT (Moon Laser Instrumentation for General relativity High-accuracy Tests), an INFN R&D experiment. This work was based on the innovative idea of replacing the Apollo and Lunokhod CCR arrays with single, large, distributed, second generation CCRs, insensitive the lunar librations, which dominate the LLR error budget with current multi-CCR arrays. A precursor test of the MoonLIGHT/LLRRA21 payload, in a synergetic effort with the LSSO project, was proposed to ASI during the Phase A Study of the MAGIA (Missione Altimetrica Gravimetrica geochImica Lunare) lunar orbiter mission. This idea is now pursued for proposed future missions to the lunar surface, like Selene-2 of JAXA<sup>2</sup> and Lunette<sup>3</sup> proposed for NASA's Discovery 2010 program, and the International Lunar Network (ILN).

INFN-LNF built the "Satellite/Lunar Laser Ranging (SLR/LLR) Characterization Facility" (SCF) and performed thermal/optical/vacuum tests in laboratory-simulated space conditions. The SCF is a unique diagnostic, optimization and validation tool of the LLR/SLR space segment. The improvement of the lunar orbit modeling is necessary to take advantage of the unprecedented mm-level accuracy now enabled by the new "Apache Point Observatory Lunar Laser ranging Operation" (APOLLO) in New Mexico. To do this we are using the "Planetary Ephemeris Program" (PEP), a versatile, powerful and opensource software package developed and maintained by the Center for Astrophysics (CfA).

---

<sup>1</sup> Contract NNX07AV62G

<sup>2</sup> Japan Aerospace Exploration Agency

<sup>3</sup> Lunar Network

## 1. LUNAR LASER RANGING

The Lunar Laser Ranging technique, as well as satellite laser ranging technique, is a time of flight measurement of a laser pulse sent by a station on the Earth to a cube corner reflector on the Moon, or on a satellite, and sent back to the station [1] [2].

Laser ranging technique, shown in Figure 1, is a very precise and cost-effective distance measurement in space.

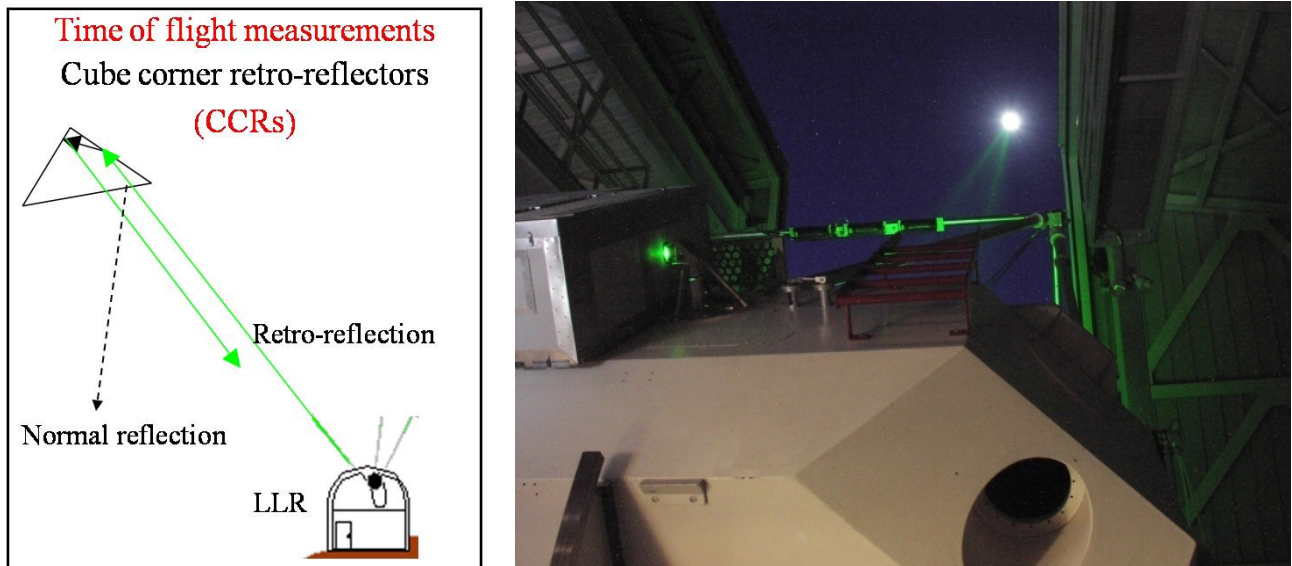


Figure 1: *Sketch of LLR technique (left) and photo of the APOLLO LLR station in operation (right).*

A CCR is a solid cube corner retroreflector, typically made of fused silica (see Figure 2).



Figure 2: *Photos of some kind of Cube Corner Retroreflectors.*

The CCRs are mounted in Laser Retroreflector Arrays (LRA), that are passive, lightweight, maintenance free, and, if built with proper thermal design and choice of materials like the Apollo ones, can provide very good performance for several decades (Figure 3).

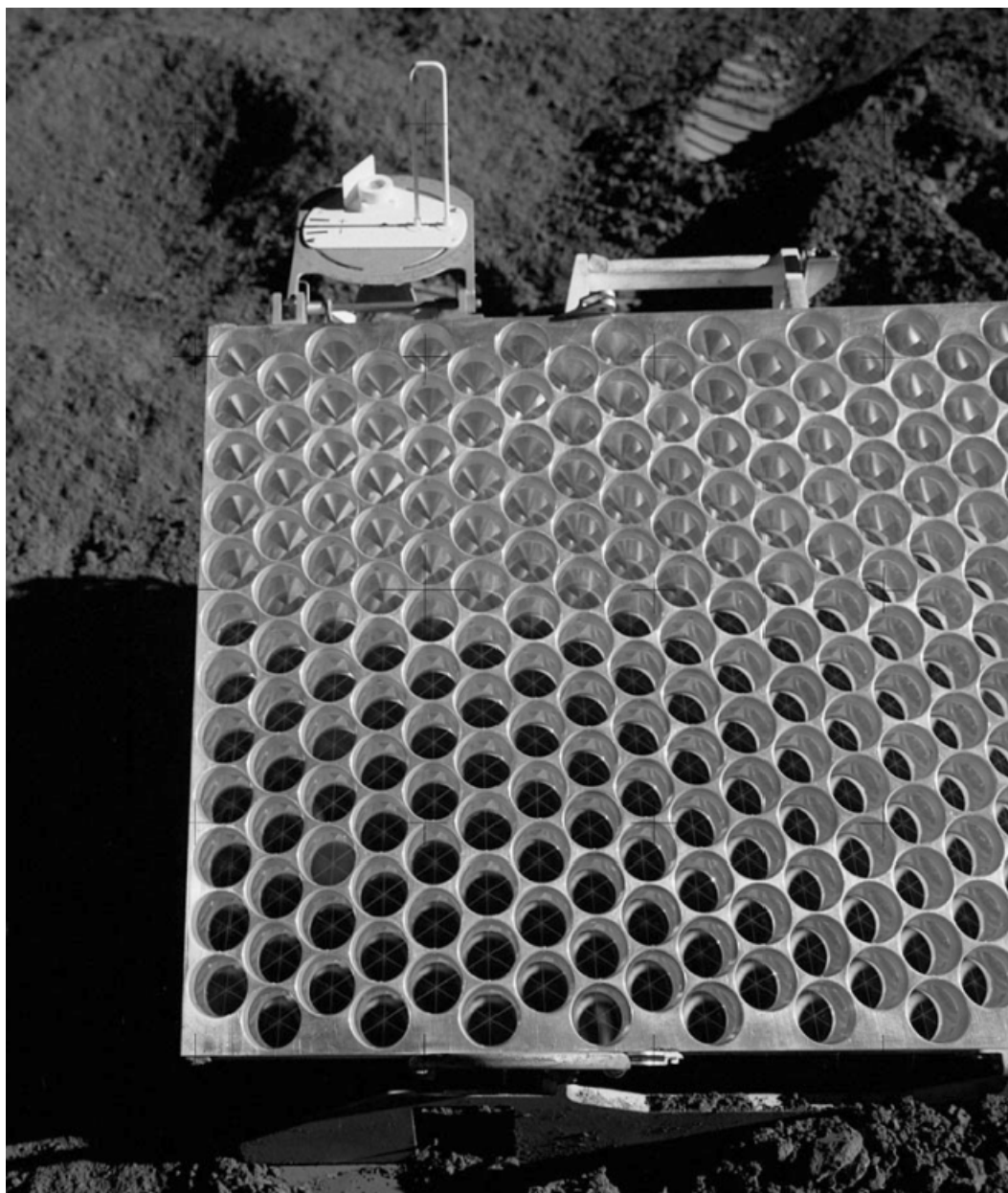


Figure 3: *The Apollo 15 Laser Retro-reflector Array.*

This was historically demonstrated with the LRAs deployed on the surface of the Moon (Figure 4) by NASA's Apollo 11, 14 and 15 missions, designed by a team led by C. O. Alley, D. Currie, P. Bender and Faller et al [1] and with the Soviet missions Luna 17 and 21 (Figure 5).

In the past 40 years, laser ranging to these arrays has provided most of the definitive tests of the many parameters describing General Relativity [3]. In addition, the analysis of the LLR data, in collaboration with some data from other modalities, has greatly enhanced our understanding of the interior structure of the Moon ([4], [5], [6], [7]). Thanks these arrays, the Earth-Moon distance is measured with an accuracy of a few cm, that is, a relative accuracy of  $10^{-10}$ - $10^{-11}$  of the Earth-Moon

distance (approximately 384,000 km). The pulse takes 1.255sec to travel, one way, the mean orbit distance. After four decades these arrays are still in operation, and are the only experiment on the Moon still producing scientific data.

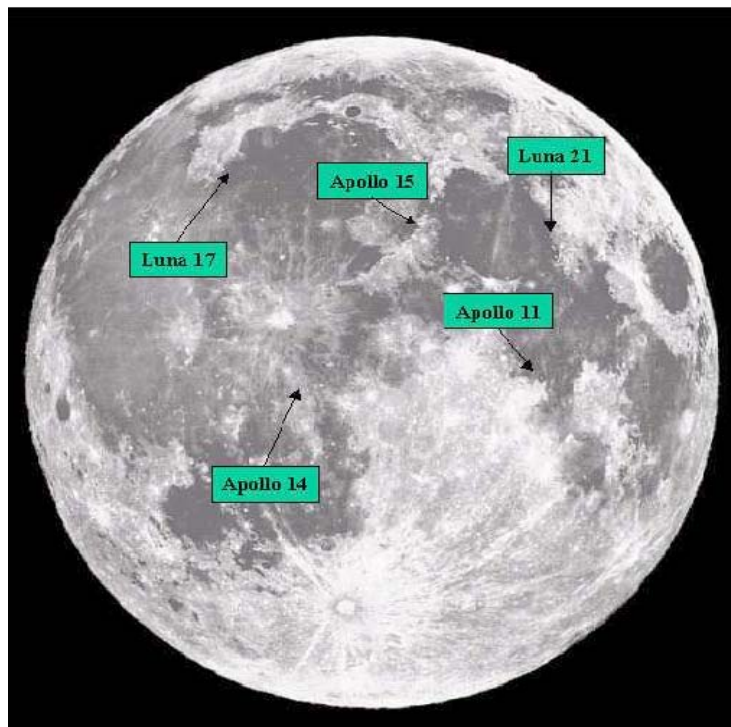


Figure 4: *Locations of the current LRAs deployed by Apollo and Luna missions.*

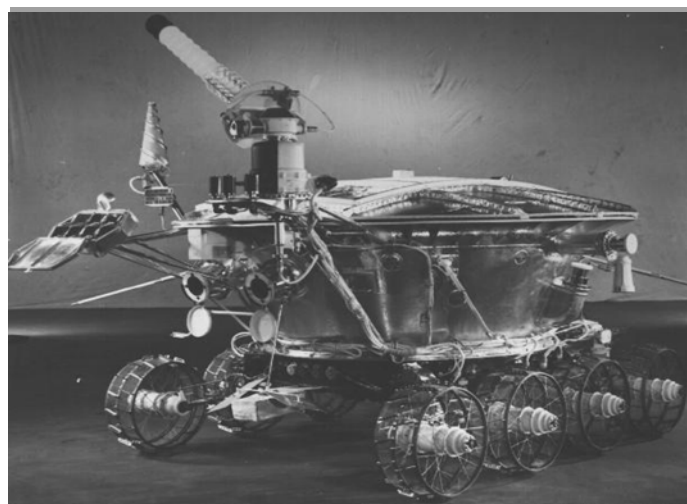


Figure 5: *Lunokhod 1 rover (carried on the lunar surface by the Luna 17) recently re-discovered by NASA's Lunar Reconnaissance Orbiter and accurately re-located by the APOLLO station.*

However over the past four decades the ground station technology has greatly improved, enhancing LLR accuracy (Figure 6). Historically the accuracy of LLR measurements is dropped from more than 30 cm, to about 2 cm, thanks to the improvement of the LLR station and their capability to records

photons. But as you can see in the Figure 6 an asymptote has been reached and we'll show the reason later.

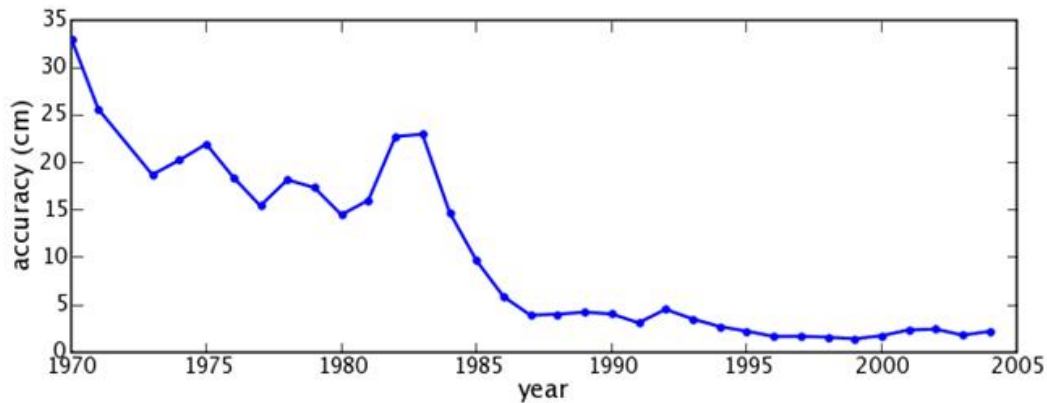


Figure 6: LLR accuracy improvements over the years and before the advent of APOLLO.

At the present time the operational LLR stations: the oldest McDonald, in Texas, CERGA<sup>4</sup>, in France and the most recently built, APOLLO, which has an instrumental precision of a few mm [8].

## 2. GENERAL RELATIVITY TESTS

These accurate Earth-Moon distance measurements have, as the main fundamental physics application, the precise test of Einstein's theory of General Relativity (GR) and of new gravitational theories in the Solar System in the weak-field slow-motion approximation. Other closely related applications, not addressed in this chapter, are the geophysical and lunar physics studies of the internal structure and formation history of the Moon.

The reason to perform this test comes from two theoretical problems until now unsolved.

1) The unification of the fundamental forces by the Standard Model of elementary particles and interactions. The Standard Model falls short of being complete, because it does not incorporate GR together with the electromagnetic, strong and weak interactions.

2) The Accelerated expansion of the Universe. The most common theory, at the moment, is to explain this accelerating universe (demonstrated by observations of very distant supernovae in 1998, see [9]) by the presence of a new component of the universe, a "dark energy", that is a sort of variant of a cosmological constant already introduced by Einstein to correct his theory and reconcile it with early observations of the expansion of the universe. No theoretical models and experiments are able to explain and describe this mysterious form of dark energy in the amount required by observations (73 percent of the total mass of the universe; while 23 percent is composed of Dark Matter, another unknown component; and the rest 4 percent comprises ordinary matter, protons, neutrons and electrons that we and the galaxies are made of). The required amount of dark energy is so difficult to reconcile with the known laws of nature that physicists have proposed alternative theories [10].

Extensions of GR have been proposed, to compare theory and experiment (see [11] for a comprehensive review). An approximation, known as the post-Newtonian limit, is sufficiently accurate to encompass most solar-system tests that can be performed at the present. The only way that one metric theory differs from another is in the numerical values of the coefficients that appear

<sup>4</sup> Centre d'Etudes et de Recherches Géodynamiques et Astronomiques

in front of the metric potentials. This Parametrized Post-Newtonian (PPN) formalism inserts parameters in place of these coefficients, parameters whose values depend on the theory under study. In the current version of the PPN formalism, ten parameters are used. Here we focus in the parameters  $\gamma$  and  $\beta$  (Table 1), used to describe “classical” tests of GR; they are the most important and the only nonzero parameters in GR [11].

Parameter	What it measures relative to GR	Value in GR	Value in PPN formalism
$\gamma$	How much spacecurvature produced by unit rest mass?	1	$\gamma$
$\beta$	How much “nonlinearity” in the superposition law for gravity?	1	$\beta$

Table 1: *PPN parameters and theirs meanings.*

Current best measurement of  $\gamma$  comes from the Cassini mission ([12]):

$$\gamma = 1 + (2.1 \pm 2.3) \times 10^{-5}$$

The measurement of  $\beta$  is described in detail in the following (science measurement n. 3).

Searches for new gravitational physics including spacetime torsion have been performed. March, Bellettini, Tauraso and Dell’Agnello in [13] and [14] search for new gravitational physics phenomena based on the Riemann-Cartan theory of General Relativity including spacetime torsion. Starting from the parametrized torsion framework of Mao, Tegmark, Guth and Cabi [15] (see also [16]), they analyze the motion of test bodies in the presence of torsion, and in particular they compute the corrections to the perihelion advance and to the orbital geodetic precession of a satellite. They describe the torsion field by means of three parameters  $t_1, t_2, t_3$ , and they make use of the autoparallel trajectories, which in general may differ from geodesics when torsion is present. They derive the equations of motion of a test body in a spherically symmetric field, and the equations of motion of a satellite in the gravitational field of the Sun and the Earth. They calculate the secular variations of the longitudes of the node and of the pericenter of the satellite. The computed secular variations show how the corrections to the perihelion advance and to the orbital de Sitter effect depend on the torsion parameters. To test that predictions, they use the measurements of the Moon geodetic precession from lunar laser ranging data, and the measurements of Mercury’s perihelion advance from planetary radar ranging data. These measurements are then used to constrain suitable linear combinations of the torsion parameters (Figure 7).

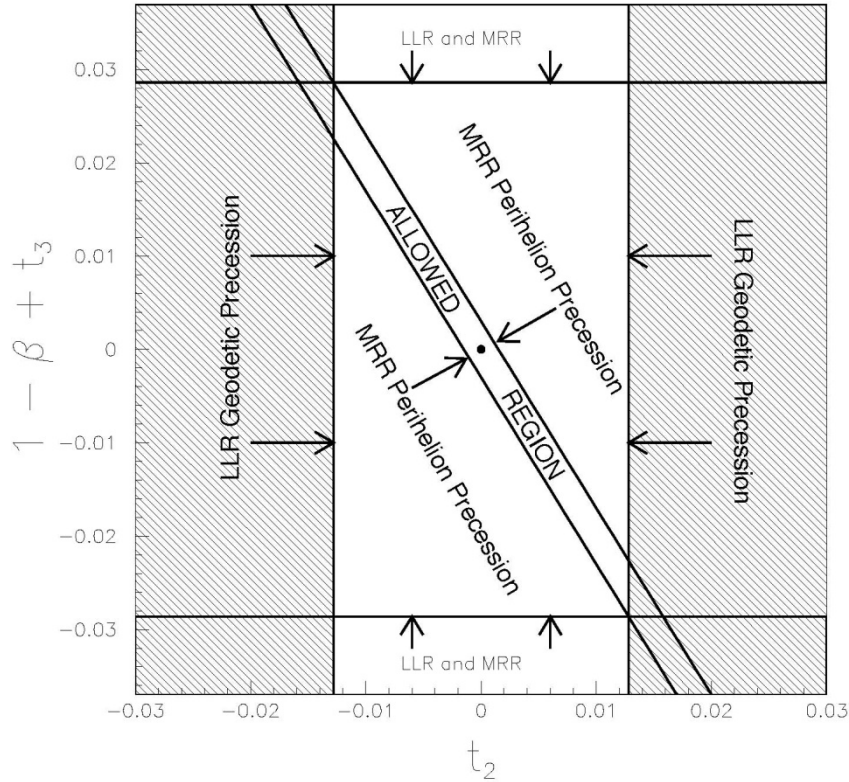


Figure 7: Constraints on  $t_2$  and the linear combination  $(1-\beta)+t_3$  from LLR and Mercury radar ranging (MRR), indicated by the arrows. For example, the hatched area is the region excluded by LLR only. General Relativity corresponds to  $\beta - 1 = t_2 = t_3 = 0$  (black dot).

We have analyzed why is important to study the GR theory and now we summarize past efforts to test the GR, started from Einstein himself.

The history of experimental relativity went through several phases, starting from its birth in the 1919. At that time Einstein himself did calculate observable effects of general relativity, such as the perihelion advance of Mercury, which he knew to be an unsolved problem, and the deflection of light, which was subsequently verified. After that, from 1920 to 1960, there was a temporary stop as long as started a renew interest in it thanks to several astronomical discoveries, i. e. quasars, pulsars and cosmic microwave background radiation (CMB). The latter period started from 1960 with the confirm of the gravitational frequency shift of light and ended, in 1980, with the reported decrease in the orbital period of the Hulse-Taylor binary pulsar at a rate consistent with the GR prediction of gravity wave energy loss. The results all supported GR, and most alternative theories of gravity fell by the wayside. Since 1980, the field has entered what might be termed a Quest for Strong Gravity. Today, experimental gravity is a major component of the field, characterized by continuing efforts to test the theory's predictions, to search for gravitational imprints of high-energy particle interactions, and to detect gravitational waves from astronomical sources [11].

Many of the remaining interesting weak-field predictions of the theory are extremely small and difficult to check, in some cases requiring further technological development to bring them into detectable range. The possibility to verify the GR predictions has been extended by the LLR

technique. In fact, almost all of the most accurate tests of General Relativity are currently derived from LLR to the Apollo arrays ([17], [18], [19], [20]): PPN parameters  $\beta$  and  $\gamma$ , Weak and Strong Equivalence Principle (WEP/SEP), time variation of the gravitational constant ( $\dot{G}$ ), deviation from the inverse square law and the geodetic precession (parameter  $K_{GP}$ ).

These parameters are now measured thanks to an LLR accuracy of a few centimeters (Table 2). Future improvements will come from the mm-accurate APOLLO data and from the deployment of 2<sup>nd</sup> generation LLR payloads (see section 3).

Science Measurement	1 <sup>st</sup> Generation (Apollo/Lunokhod) LLR Accuracy (cm)
Equivalence Principle (EP)	$ \Delta a/a  \sim  \Delta(M_G/M_I)  < 1.4 \times 10^{-13}$
Strong Equivalence Principle (SEP)	$ \eta  < 4.4 \times 10^{-4}$
Parametrized Post Newtonian (PPN) $\beta$	$ \beta - 1  < 1.1 \times 10^{-4}$
Variation in the gravitational constant $\dot{G}/G$	$ \dot{G}/G  < 9 \times 10^{-13} \text{ yr}^{-1}$
Geodetic Precession $K_{GP}$	$K_{GP} \sim 6.4 \times 10^{-3}$
Deviation from $1/r^2$	$ \alpha  < 3 \times 10^{-11}$

Table 2: *Current tests of GR.*

We enter into details of the single science measurements.

1) First of all the **Equivalence Principle (EP)**. It addresses the exact correspondence of gravitational and inertial masses, that is a central assumption of general relativity. Experimentally in the solar system is compared free fall acceleration of Earth and Moon towards the sun: if gravitational mass and inertial mass are not equal, then the EP is violated, consequently Earth and Moon would fall at different rates toward the sun, as you can see in the sketch in Figure 8.

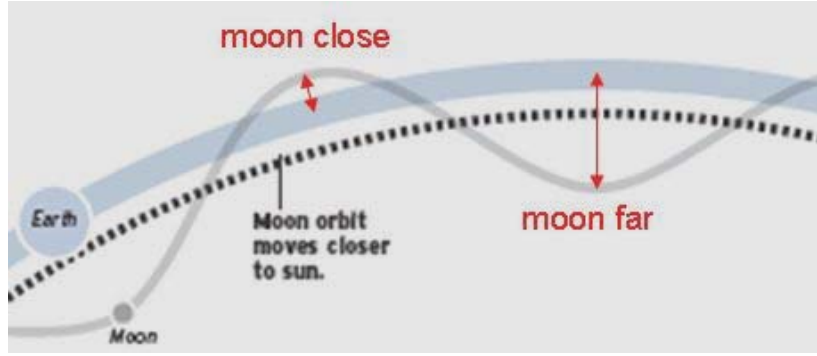


Figure 8: *Sketch of orbit changing due to eventually violation of Equivalent Principle. In blue is the Earth orbit, coincident with the average Moon orbit, but the Moon orbits the Sun, beyond the Earth, so the dotted line comes the average Moon orbit closer to the Sun, and the grey line is the path of Moon (graphic excerpt from San Diego Union Tribune).*

This difference would appear as a lunar orbit displaced along Earth-Sun line with range variation  $\Delta r \propto \cos(D)$ , (where  $D$  corresponds to 29.53 days, that is the lunar phase.  $D=0^\circ$  is the new lunar phase and  $D=180^\circ$  is the full lunar phase). Fit to LLR data, corrected for solar radiation pressure (SRP), leads to the following result:

$$\Delta(M_G/M_I) = [(M_G/M_I)_{Earth} - (M_G/M_I)_{Moon}]_{EP,LLR} = (-1.0 \pm 1.4) \times 10^{-13}$$

This difference, between the mass ratio (gravitational over inertial), of the Earth and the Moon, corresponds to:

$$\Delta r = (2.8 \pm 4.1) \text{ mm} \times \cos D = \Delta r_{LLR} - \Delta r_{SRP}$$

SRP is accounted for a posteriori, by a mathematic count performed by Vokrouhlicky in the 1997 (see [21]), and then subtracted from  $\Delta r_{LLR}$ :

$$\Delta r_{SRP} = (-3.65 \pm 0.08) \text{ mm} \times \cos D$$

If we accept the SRP count, so the error due to the solar radiation pressure is much smaller than the LLR fit error.

For example: one particular LLR fit returns  $(-0.6 \pm 4.2)$  mm (without considering the contribution of the solar radiation pressure), but SRP-corrected results is  $(3.1 \pm 4.2)$  mm [19].

2) The LLR test of EP is sensitive to both: composition-dependent (CD), i. e. the “type” of mass, (for example feather vs. hammer, this concept is addressed in the weak equivalent principle) and self-energy violations, i.e. quantity of mass, (for example big vs. small hammer, concept addressed in the strong equivalent principle). At the University of Washington (UW) was performed an laboratory EP experiment with “miniature” of Earth and Moon, in order to measure *only* CD contribution:

$$[(M_G/M_I)_{Earth} - (M_G/M_I)_{Moon}]_{WEP,UW} = (1.0 \pm 1.4) \times 10^{-13} \text{ (WEP only)}$$

From the subtraction of UW from LLR results one gets the SEP test:

$$[(M_G/M_I)_{Earth} - (M_G/M_I)_{Moon}]_{SEP} = (-2.0 \pm 2.0) \times 10^{-13}$$

This result is very important, because the strong equivalence principle can be tested only through LLR.

3) From the SEP test, carry out through the LLR technique, is also possible to gather implications on PPN  $\beta$ . SEP violation is due to self-energy contribution only; it can be expressed as:

$$\left[ (M_G/M_I) \right]_{SEP} = 1 + \eta (U/Mc^2)$$

Where  $\eta$  is an dimensionless parameter, that is a linear combination of 7 to 10 post Newtonian parameters;  $U$  is the self-energy,  $U=M^2/R$  and then  $U/M \propto M$ . Ensur from the latter proportion that to test SEP we need astronomical bodies, that is possible thanks to LLR.

Done difference between the mass ratio, gravitational over inertial, of the Earth and the Moon, is equal to done the difference between self-energy and rest-energy ratio of the two bodies:

$$\left[ (M_G/M_I)_{Earth} - (M_G/M_I)_{Moon} \right]_{SEP} = \left[ U_E/Mc^2 - U_M/Mc^2 \right] \times \eta = -4.45 \times 10^{-10} \times \eta$$

From which we obtain a result proportional to the dimensionless parameter eta. For eta we considering only the linear combination of beta and gamma parameters:

$$\eta = 4\beta - \gamma - 3 = (4.4 \pm 4.5) \times 10^{-4}$$

We took the gamma value measured by Cassini probe with the accuracy of  $10^{-5}$ :

$$\gamma - 1 = (2.1 \pm 2.3) \times 10^{-5}$$

In this way we obtain the limit of beta parameter, according to the GR prediction, that is:

$$\beta - 1 = (1.2 \pm 1.1) \times 10^{-4}$$

This is the best measurement to date.

4) Regarding the variation in the gravitational constant, this is expressed through ratio  $\dot{G}/G$ :

$$\dot{G}/G = \sigma \times (\text{Hubble constant})$$

Where:  $G$  variation can be due to expansion of the Universe;  $\sigma$  is a dimensionless parameter depending on  $G$  and cosmological model.

Test of temporal variation of  $G$  from fit of LLR data gives:

$$\dot{G}/G = (4 \pm 9) \times 10^{-13} / yr$$

The uncertainty is 83 times smaller than inverse age of the Universe (13.4 Gyr) with  $H_0 = 72$  km/sec/Mpc from WMAP<sup>5</sup>.

Any isotropic expansion of Earth's orbit conserving angular momentum mimics effect of  $\dot{G}$  on Earth's semi-major axis, i.e.,  $da/dt/a = \dot{G}/G$ . No evidence for such local ( $\sim 1$  AU) scale expansion of solar system. The error on  $\dot{G}/G$  depends on the square of time span of LLR data.

---

<sup>5</sup> Wilkinson Microwave Anisotropy Probe satellite

5) Regarding the geodetic precession this is a 3-body effect (Sun, Earth, Moon) predicted by GR (de Sitter). This effect address the precession of a moving gyroscope (the Moon orbiting the Earth) in the field of the Sun of about  $(3.00 \pm 0.02)$  m/moon orbit, that are about  $2''/\text{cy}$ , as shown in Figure 9.

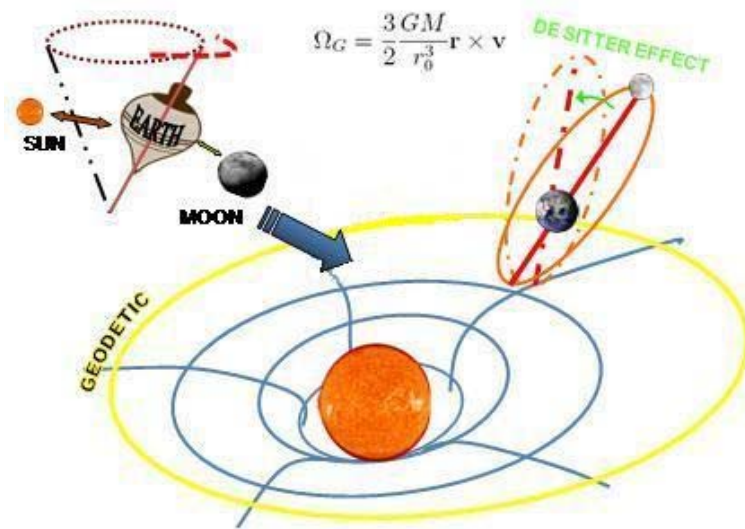


Figure 9: Sketch of the Moon precession orbiting the Earth in the Sun field.

Relative deviation of geodetic precession from GR is expressed from the  $K_{GP}$  parameter, equal to:

$$K_{GP} = -0.0019 \pm 0.0064$$

LLR data give unique science products both in relativistic gravity AND in lunar geophysics. LLR addresses both.

6) Concerning the last science measurement reported in the table 2, the deviation from  $1/r^2$ , can be roughly thought of as a generalization of an inverse-square force potential that takes into account a massive mediator or force. This would mean that instead of massless photons exchanging the force, as is the case with electromagnetism, some other particle with mass exchanges the force between two particles. At astronomical distance, gravitation might has different distance ( $r$ ) dependence, different from  $1/r^2$ .

Current limits on additional Yukawa potential:

$$\alpha \times (\text{Newtonian} - \text{gravity}) \times e^{-\frac{r}{\lambda}}$$

Where Newtonian gravity is expressed by:

$$F = G \frac{m_1 m_2}{r^2}$$

Then the Yukawa potential appears in the form:

$$V_{Yuk} = -\alpha \frac{GM}{r} e^{-\frac{r}{\lambda}}$$

Plotting values of  $\alpha$  vs. values of  $\lambda$ , we can find the graphic in Figure 10.

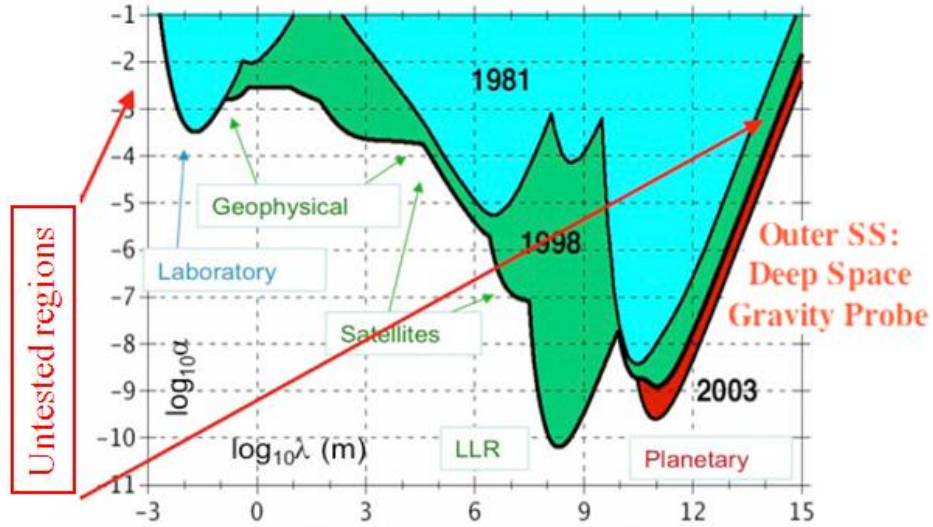


Figure 10: Measurements of Yukawa potential performed in different ways [22].

### 3. MOONLIGHT/LLRA21 PAYLOAD

In paragraph 2 we have spoken about fundamental physics tests done since now with the best LLR accuracy to date, that is about 2 cm. In Table 3 we report the improvement of the science measurement made possible thanks to the equivalent improvement in the accuracy of the measurements of one or two orders of magnitude, reaching 1 mm, or even 0.1 mm, of accuracy.

Science Measurement	1 <sup>st</sup> Generation (Apollo/Lunokhod) LLR Accuracy (~cm)	2 <sup>nd</sup> Gen. (MoonLIGHT) LLR accuracy (1 mm)	2 <sup>nd</sup> Gen. (MoonLIGHT) LLR accuracy (0.1 mm)	Time Scale - 2 <sup>nd</sup> Gen.
EP	$ \Delta a/a  < 1.4 \times 10^{-13}$	$10^{-14}$	$10^{-15}$	Few years
SEP	$ \eta  < 4.4 \times 10^{-4}$	$3 \times 10^{-5}$	$3 \times 10^{-6}$	Few years
$\beta$	$ \beta - 1  < 1.1 \times 10^{-4}$	$10^{-5}$	$10^{-6}$	Few years
$\dot{G}/G$	$ \dot{G}/G  < 9 \times 10^{-13} \text{yr}^{-1}$	$5 \times 10^{-14}$	$5 \times 10^{-15}$	~5 years
Geodetic Precession $K_{GP}$	$6.4 \times 10^{-3}$	$6.4 \times 10^{-4}$	$6.4 \times 10^{-5}$	Few years
$1/r^2$ Deviation	$ \alpha  < 3 \times 10^{-11}$	$10^{-12}$	$10^{-13}$	~10 years

Table 3: Improvement of the science measurement thanks to the improvement in the accuracy of the measurements of one or two orders of magnitude, (reaching 1 mm or even 0.1 mm of accuracy).

At this point, after the building of the best station, APOLLO, in New Mexico, the main uncertainty is due to the multi-CCR arrays. The Apollo arrays now contribute a significant portion of the ranging errors. This is due to the lunar librations, which move the Apollo arrays, since that have dimensions of 1 square meter, for the Apollo 15, and half square meter, for the Apollo 11 and 14. In this paragraph we will describe the MoonLIGHT/LLRRA21 payload to improving gravity tests and lunar science measurements. This project is the result of the collaboration of two teams: the one in the USA, led by Douglas Currie of the University of Maryland, and the Italian one led by INFN-LNF. We are exploring improvements both the instrumentation and the modeling of the CCR.

First of all, it is important to understand the limitation of arrays with a multi-CCR structure located on the lunar surface. The main problem that affects the Apollo arrays is the lunar librations, in longitude, that results from the eccentricity of the Moon's orbit around Earth. During the lunar phase, 27 days, the Moon's rotation alternatively leads and lags its orbital position, of about 8 degree. Due to this phenomenon the Apollo arrays are moved so that one corner of the array is more distant than the opposite corner by several centimeters. Because the libration tilt, the arrays increase the dimension of the pulse coming back to the Earth (see Figure 11). The broadening of the impulse will be greater proportionally to the array physical dimensions and to the Moon-Earth distance increase (in the position in which the libration phenomena are at the peak). Therefore for the biggest Apollo 15 the enlargement is about 30 cm, instead is about 15 cm for Apollo 11 and Apollo 14 arrays. In agreement with this relationship, the pulse enlargement correspond to a time flight increase:

- ± 0.5 nanoseconds for Apollo 15 (see Figure 31);
- ± 0.25 nanoseconds for Apollo 11 and Apollo 14.

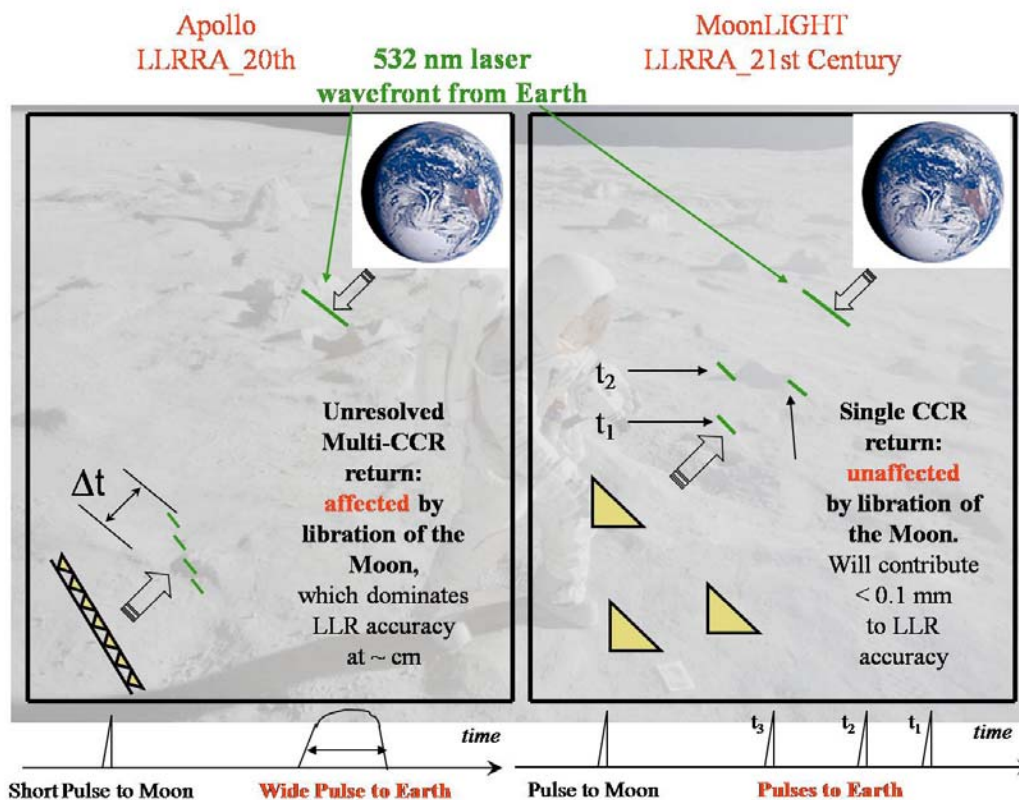


Figure 11: Comparison between 1<sup>st</sup> and 2<sup>nd</sup> generation LRAs. The librations tilt the arrays on the left, but the single big CCRs are unaffected, on the right. So we have single short pulses coming back.

So the accuracy of the ranging measurements cannot go below few centimeters (for a single normal point). At the present without hardware improvement, one can only progress by timing an extremely

large number of single photoelectron returns to reduce the errors by the root mean square of the single photoelectron measurement error [8].

In order to solve this problem, the SCF group, in collaboration with the University of Maryland, indicates a new design of lunar CCR, named the 2<sup>nd</sup> generation LLR, whose performance is unaffected not only by lunar librations, but also by regolith motion, due to its very large thermal cycle. The idea that we propose is: moving from an array of multiple-small-CCR, everyone with 3.8 cm of front face diameter, to a series of single big CCR, each with 10.0 cm of front face diameter, deployed separately on the lunar surface (see Figure 12).



Figure 12: *Photos of Apollo, 1<sup>st</sup> generation and MoonLIGHT/LLRRA21, 2<sup>nd</sup> generation CCR.*

Instead of having a single pulse, spread by the array and the libration effect, we will have single short pulses coming back with the same dimensions as the incoming one (see Figure 11), with a final LRA ranging accuracy below 10  $\mu\text{m}$ . When the new CCRs will be placed on the lunar surface, will make sense improve the stations capabilities.

To summarize, in the past there was a fat laser pulse fired from the Earth station, bigger than array dimensions, that dominated the measurement uncertainty. Now there is average size laser pulse, but still large array, so that the measurement uncertainty is dominated by the array; in the future, with MoonLIGHT/LLRRA21, there will be a single CCR unaffected by librations. The measurement uncertainty will be dominated by laser pulse, but the modern technology can do shorter laser pulses (Figure 13).

A possibility of further development of the MoonLIGHT/LLRRA21 payload may come from the INFN-LNF and UMD participation to the international mission Lunette, proposed for the Discovery 2010 NASA program. Lunette is a dual-lander mission to the Moon to study early planetary differentiation, with C. Neal as Principal Investigator. The NASA decision for Phase A selection is expected in the first part of 2011. INFN-LNF can take part in this mission thanks to the INFN MoonLIGHT/LLRRA21 R&D experiment, with ASI's support that will be granted if the mission will be approved. Other opportunities for deployment of our payload come from the International Lunar Network (ILN), a cooperative effort designed to coordinate individual lunar landers in a geophysical network on the lunar surface (see also the conclusive section 8).

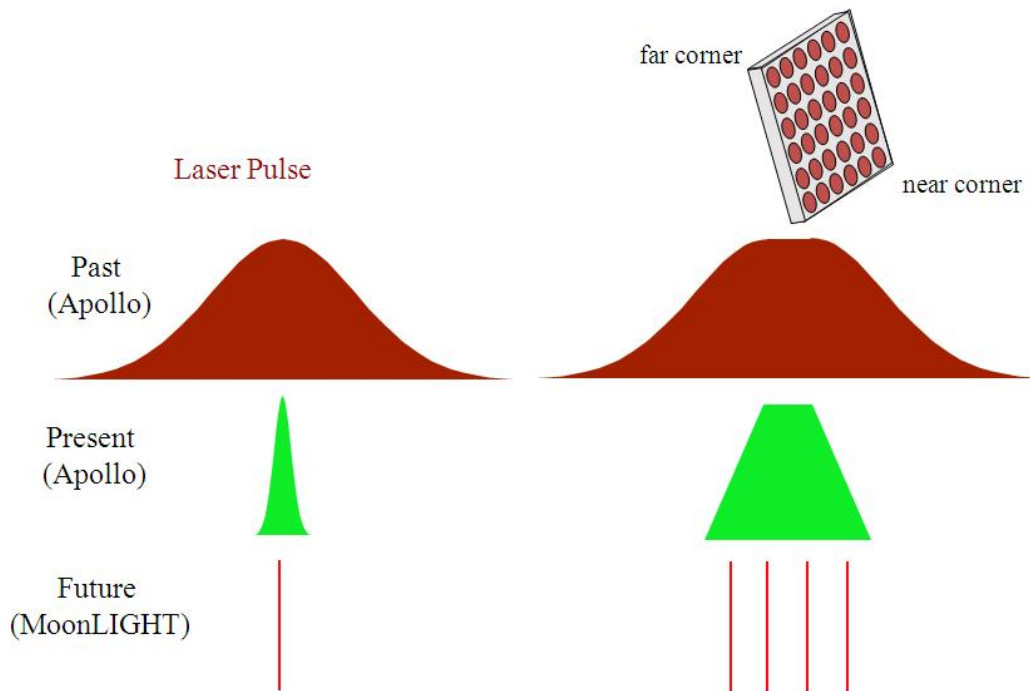


Figure 13: In the figure is shown which dominates the measurement uncertainty between laser pulse size fired and retroreflected; in the top horizontal stripe is shown the situation in the past; the middle stripe shows the currently one and the bottom the future possible situation with MoonLIGHT/LLRA21 CCR. (Photo courtesy of S. Merkowitz [23]).

In order to improve the ranging measurement we have to investigate the technical and fabrication challenges of MoonLIGHT/LLRA21, through thermal/optical simulations and vacuum chamber tests performed at the INFN-LNF SCF, as shown in the section 4. Besides the simulations we performed thermal and optical vacuum chamber tests to further validate the design issues.

#### 4. SATELLITE/LUNAR CHARACTERIZATION FACILITY (SCF)

Starting from 2004 INFN invested resources and manpower to build and start the operation of the *Satellite/Lunar Laser Ranging* (SLR/LLR) Characterization Facility (SCF) in Frascati, near Rome, dedicated to the space calibration of the thermal properties and the laser ranging response of laser retro-reflector arrays (LRAs) in accurate laboratory-simulated space conditions (see [24] for detailed description). A schematic view of the SCF is shown in Figure 14.

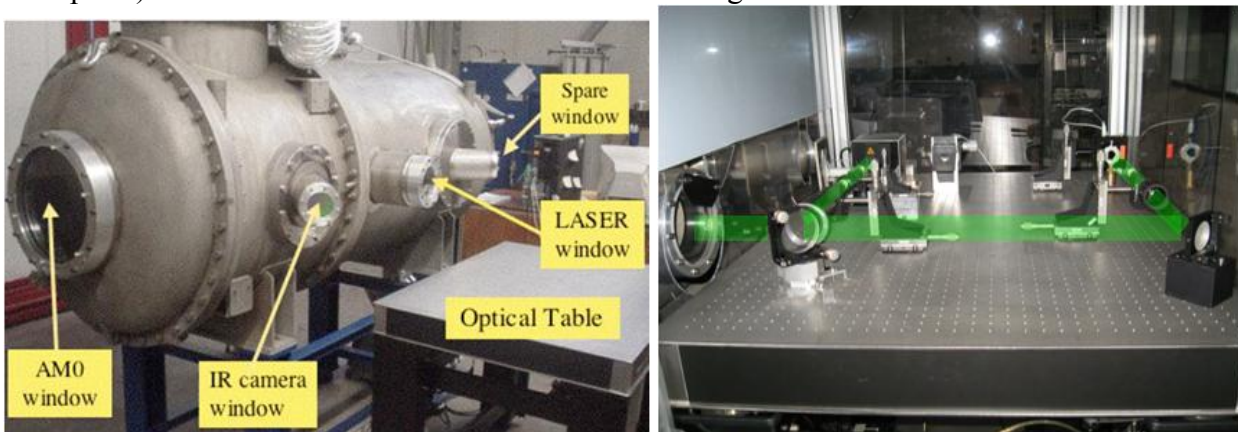
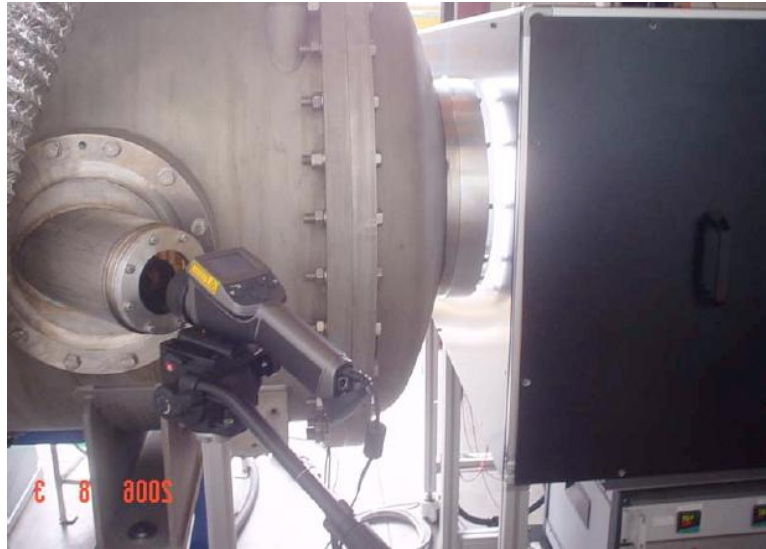


Figure 14: Left: SCF cryostat. Right: optical table for laser FFDP tests.

The size of the steel cryostat is approximately 2 m length by 0.9 m diameter. The inner copper shield is painted with the Aeroglaze Z306 black paint (0.95 emissivity and low out-gassing properties) and is kept at  $T = 77$  K with liquid nitrogen. When the SCF is cold, the vacuum is typically in the  $10^{-6}$  mbar range. Two distinct positioning systems at the top of the cryostat (one for roto-translation movements in the plane of the prototype and one for spherical rotations and tilts) hold and move the prototype in front of the Earth infrared Simulator (ES, inside the SCF), the Solar Simulator (SS), the infrared (IR) camera and laser, all located outside the SCF; see Figure 14 and Figure 15.



*Figure 15: Photos of SS and IR camera in operation.*

The SS beam enters through a quartz window ( $\sim 37$  cm diameter,  $\sim 4$  cm thickness), transparent to the solar radiation up to 3000 nm. A side Germanium window at  $45^\circ$  with respect to the SS beam allows for the acquisition of *thermograms* of the LRA with an IR digital camera (both during the ES/SS illumination and the laser interrogation phases). The SS (from [www.ts-space.co.uk](http://www.ts-space.co.uk)) provides a 40 cm diameter beam with close spectral match to the Air Mass Zero (AM0) standard of 1 solar constant in space ( $1366.1$  W/m $^2$ ) in the range 400-1800 nm; see Figure 16.

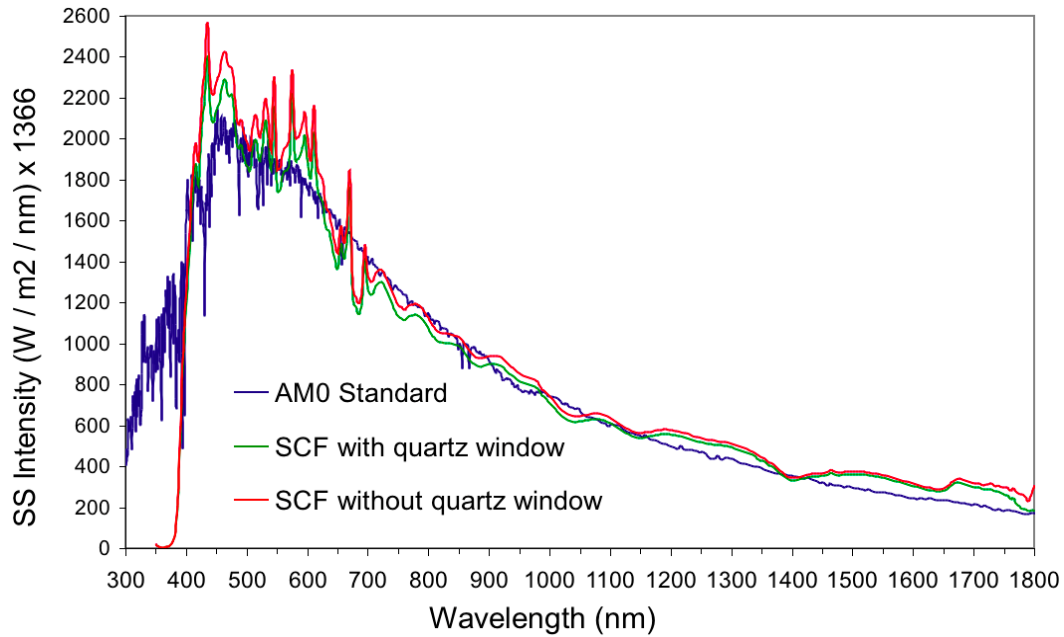


Figure 16: SCF SS spectrum with and without quartz window, compared to the AM0 standard.

The uniformity is about  $\pm 5\%$  over an area of 35 cm diameter. The spectrum is formed from a metal halide (HMI) arc lamp (UV-V; 6 KW), together with a quartz halogen, tungsten filament lamp (Red-IR; 12 KW). The SCF spectrum is also in reasonable agreement with the AM0 over  $\lambda = 1500 \text{ nm} - 3000 \text{ nm}$  [24].

The absolute scale of the SS intensity is established by exposing the SS beam to a reference device, the *solarimeter*, which is a standard [www.epply.com](http://www.epply.com) thermopile (calibrated blackbody), accurate and stable over 5+ years to  $\pm 2\%$ . The ES is a 30 cm diameter disk painted with Aeroglaze Z306, kept at the appropriate temperature (260-280 K) and distance from the satellite prototype, in order to provide the CCRs with the same Earth viewing angle in orbit ( $\sim 60^\circ$  for LAGEOS, the two LASER GEodynamics Satellites).

The temperature data acquisition consists of an IR camera for non-invasive, high spatial granularity measurements (FLIR ThermaCAM® EX320, 320×240 pixels) and class-A PT100 probes with 4-wire readout. The PT100s are used to calibrate the IR camera. They are also used below 250K, outside the IR camera working range. SCF photos are shown in Figure 14: the left IR camera window, the central window for laser measurements and the right spare window. The SS beam enters from the left through the AM0 window. The specs of the LASER window are: fused silica material; 120 mm clear and optical aperture, 38 mm thickness, good surface roughness quality (20–10 in scratch–dig units), deformations of the transmitted wavefront  $< \lambda/20$ , and anti-reflective coating on both sides (reflectivity  $\leq 0.3\%$  for  $\lambda = 532$  and 632.8 nm).

Each CCR will be first exposed to the Sun and the Earth simulators and its thermogram taken. Then, the CCR will be rotated at  $90^\circ$  in front of the LASER window to acquire its FFDP.

#### 4.1 Measurements of Far Field Diffraction Patterns (FFDPs)

The basic industrial acceptance test of the CCR optical performance is the measurement of the absolute angular size, shape and optical cross section of single-CCR FFDPs with linearly polarized continuous wave lasers [25].

The horizontal and vertical polarization components of each FFDP are recorded separately. This is particularly important for uncoated CCRs, whose FFDPs depend strongly on the orientation of the input linear polarization. No dependence is expected for coated CCRs. Our laser beam profilers are

two 12-bit, 2 Mega-pixel CCD cameras read-out through Firewire or USB with a PC. FFDPs are acquired with the CCR in Air and Isothermal Conditions (AIC). The absolute angular scale of the optical circuit is calibrated with the double-slit method to test the consistency of each CCR FFDP with its nominal Dihedral Angle Offsets (DAO expresses in arcsec or with the symbol  $\theta$ ). The latter are related to the satellite velocity aberration, which is determined by its orbital altitude (velocity). The lack of knowledge of the DAO specifications makes the modeling of the optical FFDP and, especially, its variations due to thermal effects, extremely difficult and unreliable. We also measured the FFDP intensity relative to the Airy Peak, using reference flat mirrors of known reflectivity and good optical quality. FFDP measurements were modeled with CODEV, an optical ray-tracing software package by O.R.A., Inc. The Dihedral Angle Offsets are strictly related to the satellite and lunar *velocity aberration* (Figure 17), which is in turn determined by its orbital altitude.

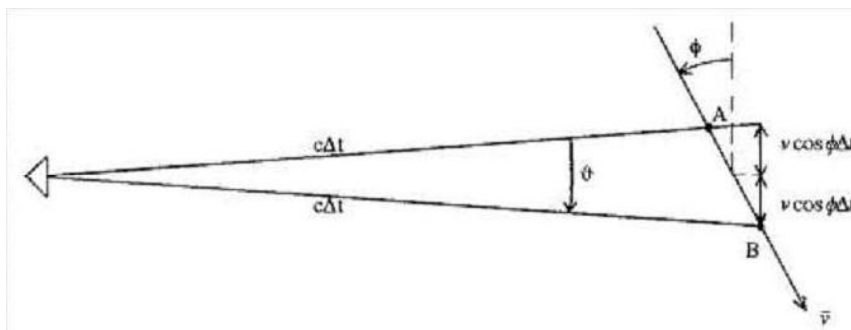


Figure 17 *Velocity Aberration sketch.*

The problem is referred to the relative movement of the CCR, on the satellite or on the Moon, round the Earth during the laser pulse time flight. It is needed to study the FFDP in order to understand in which place the laser pulse retroreflected by the CCR will reach the starting station, where is the CCD able to catch the incoming photons.

The velocity aberration for the Moon is about  $4 \mu\text{rad}$ . In this case the best choice is a  $0,0''$ ,  $0,0''$ ,  $0,0''$  (in arcsec) dihedral angle offset, because in the FFDP space is located in the central peak, (see Figure 18, [26]). The velocity aberration for the altitudes of Global Navigation Satellite System constellations is  $20$ - $25 \mu\text{rad}$ .

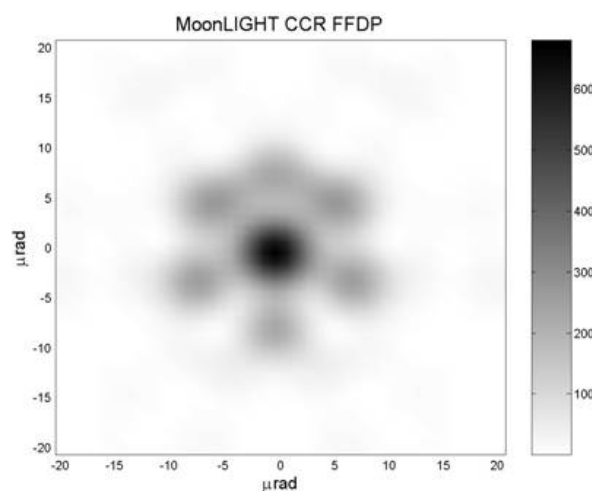


Figure 18: *Simulation of the MoonLIGHT/LLRRA21 CCR FFDP, done with the CODEV software.*

## 4.2 Simulation Software Suite

SCF measurements are also modeled with thermal and optical simulations done with: Autocad Inventor (solid modeling) and ANSYS (FEM analysis), for the thermal part and CODEV and MATLAB, for the optical part.

1. For satellite and lunar thermal analysis we adopted since 2005 a specialized suite by C&Rtech, used by several space agencies and industries: (i) Thermal Desktop, the CAD-based geometric thermal modeler, (ii) RadCad, the radiation analysis module, (iii) Sinda-Fluint, the solver and orbital simulator (TRS). TRS can handle satellites and lunar with up to 20,000 FEM nodes and a generic satellite spin and orbit configuration. It also provides the thermal inputs and orbital motions of the Sun, Earth, Moon and other planets of the solar system.

2. Optical design and analysis software: CODEV, by ORA. Note that TRS has built-in provisions for integration with CODEV. With ORA, we are developing an integrated thermal and optical analysis of CCRs in space. Always with this software we can simulate the CCR dihedral angle offset to compare the simulated value with the nominal one. Besides we use in-house software to complete the data analysis and plot comparisons of simulations versus measurements of the average intensity versus the velocity aberration.

## 5. SCF-TEST OF THE MOONLIGHT/LLRRA21 CCR

Now we apply the SCF test and subsequently analysis to the CCR concept of MoonLIGHT/LLRRA21 [24] [27]. The CCR for LLRRA-21 has the same design style as the Apollo cubes (circular front face, with tabs on the non reflecting surfaces to help its emplacement inside the housing); however, it is much bigger than its predecessor, for the reasons explained above; the absolute intensity in return (optical cross section) would replace half of the Apollo 11 array intensity. Despite this loss in the intensity of the return, it should be noticed that with the APOLLO station, the efficiency of LLR is increased, and even with 50% reduction in the intensity of the return, a very good measurement is guaranteed.

The angles between the three back surfaces have a specification on the offsets of 0 arcsec, as Apollo CCRs, though with a more challenging tolerance of  $\pm 0.2$  arcsec. Fabrication, with certification of space qualification, has been commissioned to ITE Inc. of Beltsville, MD (see Figure 19).

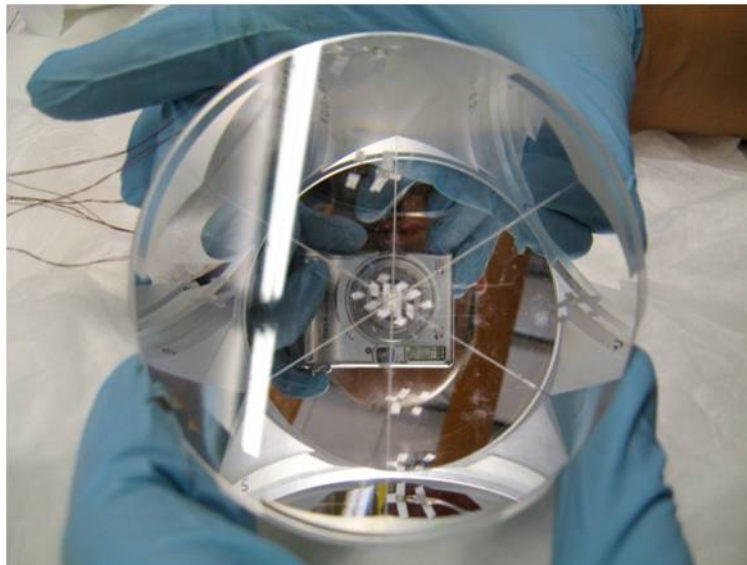


Figure 19: *MoonLIGHT/LLRRA21 photo.*

To achieve this configuration we have addressed three main challenges: technical, fabrication and thermal/optical performance.

### 5.1 Technical challenges of LLRRA-21

To achieve the goal of submillimetric accuracy beyond to provide adequate laser return to earth-based ground stations, as we explain in the previous sections, we need to be stable over long term with respect of mass of the Moon. To do this we addressed three main technical/engineering challenges:

- Fabricate a large CCR with adequate homogeneity and that meet the required tolerances, mentioned in section 4.
- Thermal control to reduce thermal gradients inside the CCR to acceptable levels. Thermal gradients produce index of refraction gradients, which cause beam spread and low return.
- Emplacement goal of long-term stability of 10  $\mu\text{m}$  with respect to the Center of Mass of the Moon.

### 5.2 Fabrication challenge

The large diameter of the CCR introduces a great challenge in its fabrication, the availability of such material of the required homogeneity, the fabrication and polishing procedures and the measurement methods. The angle between the three back reflecting faces, which govern the shape of the pattern, have a more challenging tolerance of  $\pm 0.2$  arcsec; this is more restrictive by a factor of 2.5 than the current state of the art for SLR CCR fabrication. The material choice is primarily driven by three requirements:

- extremely uniform index of refraction (very good homogeneity)
- resistance to darkening by cosmic radiation
- low solar radiation absorption

To satisfy these requirements, this CCR has been fabricated with SupraSil 1. For the next generation of CCRs, LLRRA-21, we plan to use SupraSil 311 which has even better homogeneity.

### 5.3 Thermal/optical performance challenges

The Figure 18, shown in the section 4, is a simulation of the FFDP of the LLRRA-21 (performed with the software CODEV) according to its dimensions and angle specifications; at the correct velocity aberration the intensity (calculated in optical cross section) should have a value which guarantees that enough photons come back to the ground station. The optical cross section ( $\sigma_{CCR}$ ) is an intrinsic characteristic of CCRs or LRAs (see [24] for a description), and it's defined as follows:

$$\sigma_{CCR} = I_{CCR/MIRR}(\theta_x, \theta_y) 4\pi \left( \frac{A_{CCR}}{\lambda} \right)^2$$

$I_{CCR/MIRR}$  is the intensity of the FFDP of the CCR, at a certain point of the  $(\theta_x, \theta_y)$  plane, referred to a perfect mirror of the same aperture as the CCR,  $\lambda$  is the laser wavelength and  $A_{CCR}$  is the CCR's area.

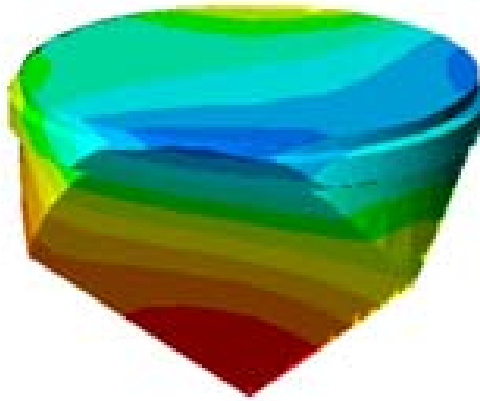


Figure 20: *A typical distribution of temperature in the CCR for a given set of conditions. This image is one in a series of day by day temperature distributions through a lunation. The temperatures illustrated by the colors range from 185.7°K to 186.8°K.*

One of the most critical challenges of this new model is the issue of the thermal gradient, see Figure 20. Since the index of refraction of the fused silica depends upon temperature, a thermal gradient inside the CCR will cause the index of refraction to vary within the CCR and thus modifying the FFDP. In Figure 21, is represented the average intensity over the velocity aberration for the LLRRA-21 at Standard Temperature and Pressure (STP). At the velocity aberration for the Moon, about 4 $\mu$ rad, we will test thermal perturbations and, if needed, develop an optimized design to control the drop of FFDP intensity to an acceptable level.

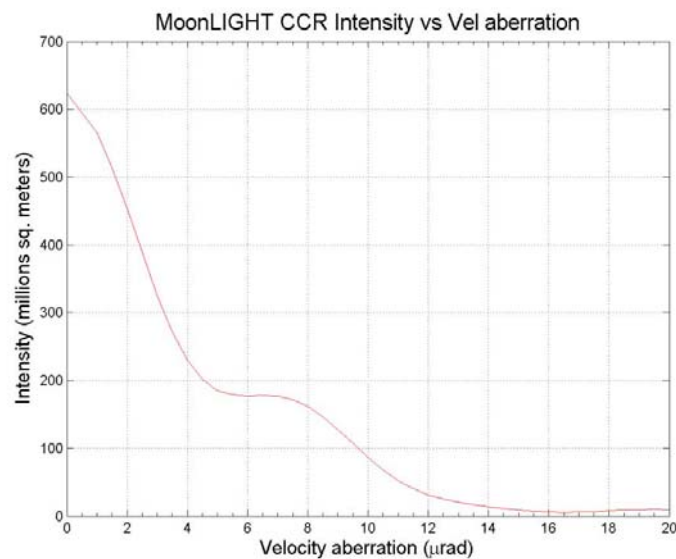


Figure 21: *Average intensity over velocity aberration of an unperturbed MoonLIGHT/LLRRA21 CCR.*

For this reason we need to understand in detail how the external factors heat the CCR and in what magnitude, either on the Moon. This is accomplished using dedicated programs developed in parallel at LNF and UMD.

There are three primary sources of heat that causes thermal gradients; here we briefly describe their effect:

- *Absorption of solar radiation within the CCR:* during a lunar day, the solar radiation enters the CCR and portions of this energy are absorbed by the fused silica. Since the different wavelengths in the solar radiation are absorbed with different intensity, according to fused silica absorptivity characteristic, the heat is deposited in different parts of the CCR.
- *Heat flux flowing through the mechanical mounting tabs:* if the CCR is at a temperature that is different than the housing temperature there will be a flux of heat passing into (or out of) the CCR through the holding tabs. Conductivity of the mounting rings should be reduced.
- *Radiation exchange between the CCR and the surrounding pocket:* in the case of the Apollo LRAs, the back surfaces of the CCRs view the aluminum that makes up the housing, machined with a relative high emissivity/absorptivity. If the temperatures of the CCR and the aluminum are different there is a radiation exchange of thermal energy, which in turn causes a flux in the CCR as the heat exits out of the front face to cold space. In the Apollo array this is not been a serious issue, but the bigger dimensions of the LLRRA-21 complicate things, and we need to reduce this effect. Thus we enclose the CCR into two thermal shields, with a very low emissivity (2%), that should prevent this radiative heat flow. Thermal simulations performed on the current configuration show that currently the variation of the  $\Delta T$  between the front face and the tip of the CCR is within 1K. We are still proceeding to optimize this further, both with optical design procedures and with thermal stabilization of the overall housing.

#### 5.4 Current housing design

We are successively refining our design upon maximizing the overall performance by jointly optimizing the effects of the various different phenomena that affect the overall performance. This has been addressed using the computer simulations described in a section 4 and using the data obtained with the SCF measurements. This addressed both the design for the robotic emplacement and the use of the 100 mm solid CCR in the MAGIA mission and/or in the ILN Anchor nodes and/or any other similar geophysical surface mission. Note that the deployment scheme with a rover (like the one suggested by ASI) or a lander (like the one now considered by ESA) will vary. Thus we illustrate the inner thermal shield in Figure 22 and current payload design, in Figure 23, that is the configuration that was used for the above simulations and for the early tests, and the sun shade drawing and photo in Figure 24.

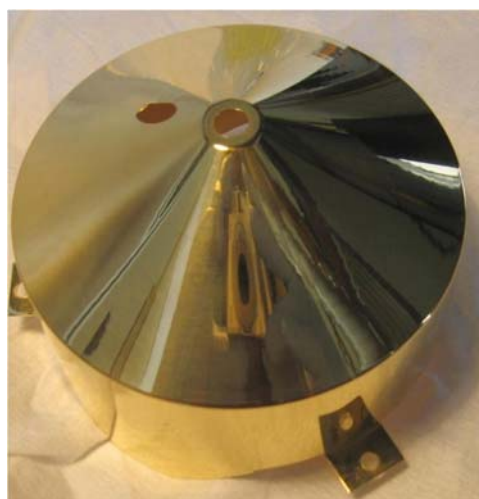


Figure 22: *Photo of the inner thermal shield.*

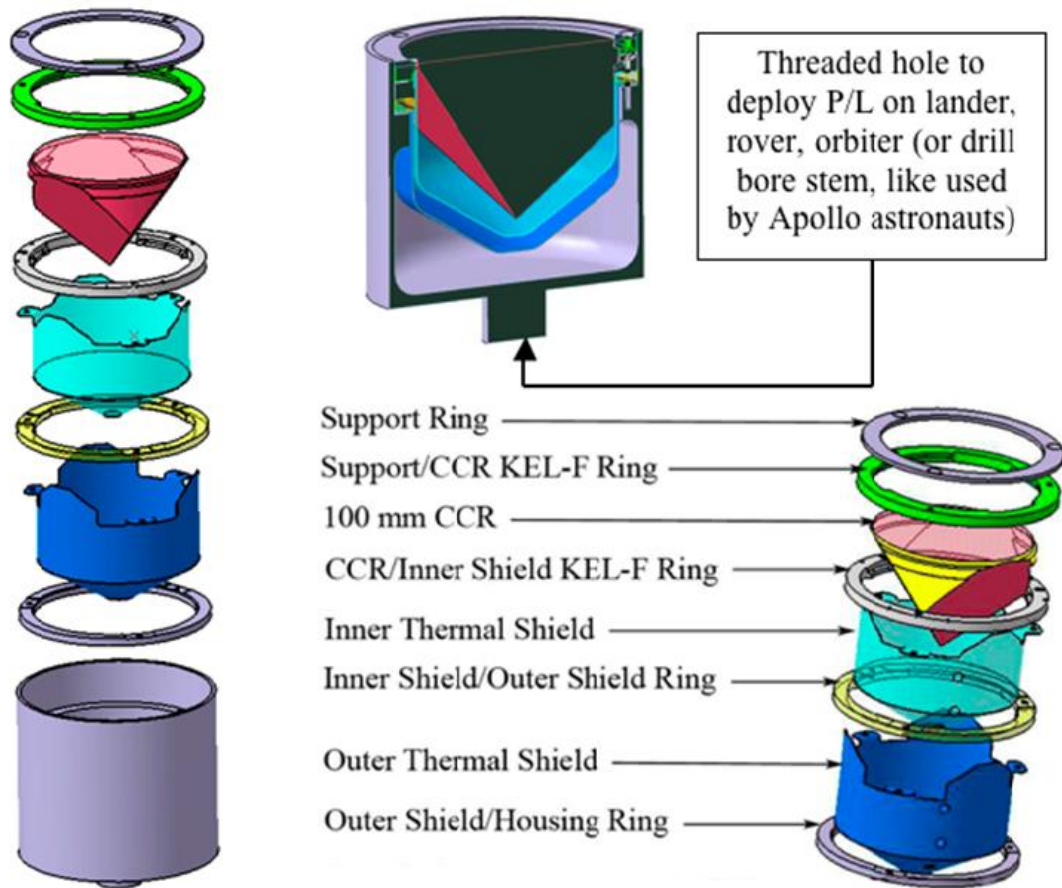


Figure 23: Views of current design of MoonLIGHT-ILN/LLRRA21 CCR with its internal mounting elements and outer metal housing.

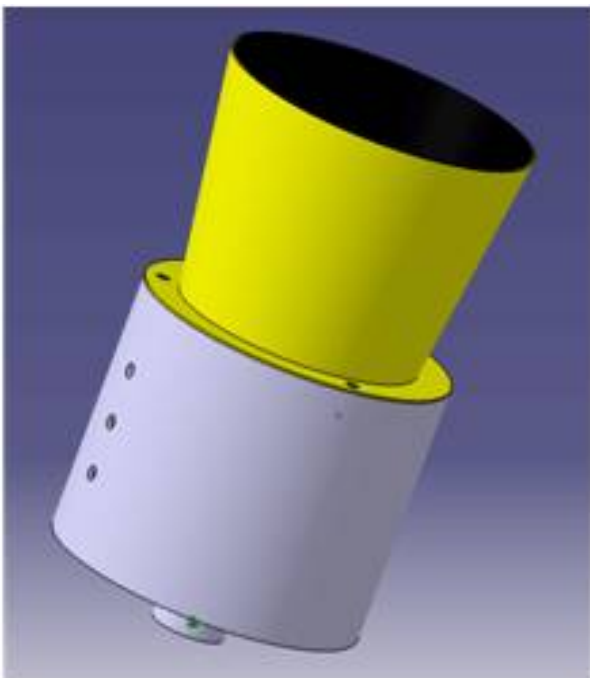


Figure 24: On the left: sun shade drawing; on the right: sun shade photo.

This is the current payload design from the top to the bottom of the exploded view there are the support ring one in aluminum and the other in KEL-F. The Suprasil1 CCR, two gold thermal shield, inner and outer. And finally the housing with threaded hole to deploy payload on lander or on rover or on orbiter. (KEL-F is a kind of plastic, with low thermal expansion and low hygroscopic potential). This design has also been proposed to the Italian Space Agency for a precursor test on the MAGIA lunar orbiter (Phase A study, see [28]), which will carry our 100 mm CCR into lunar orbit (if it receives final approval).

At last we show you two photos of MoonLIGHT/LLRRA21 CCR Thermal-Optical-Vacuum test, performed in the end of 2010 in our SCF (Figure 25).

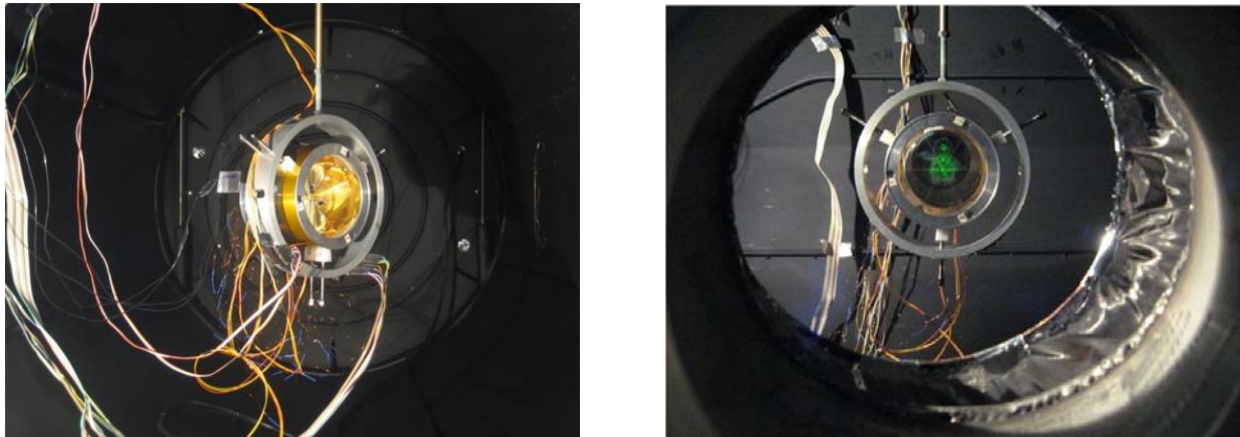


Figure 25: *SCF test of MoonLIGHT/LLRRA21 CCR. Notice, on the left, two inner gold thermal shields. While on the right you can see the green laser ( $\lambda = 532 \text{ nm}$ ), used at the SCF.*

## 6. MAGIA ORBITER

Several countries build and launched successfully Moon orbiters, as a consequence of a renewed interest in our natural satellite. First of all, in 2007, Kaguya was launched, the Japanese orbiter, closely followed, only one month later, by Chang'e, the Chinese one (launched on October 24, 2007). One year later, October 2008, was the turn of Chandrayaan, the Indian orbiter. This mission included a lunar orbiter and an impactor, as well as the following NASA's LRO<sup>6</sup> (launch date: June 18, 2009), orbiter, and LCROSS<sup>7</sup> (launched together with LRO), impactor. As regards Europe, the satellite SMART-1 (it was launched on September 27, 2003) was orbited around the Moon from 2003 to 2006.

While for Italy, in 2008 the Italian Space Agency (ASI) approved for Phase A Study five proposals presented in response to the call for "Small Missions" issued in 2007. One of these is MAGIA, whose Principal Investigator is A. Coradini (INAF-IFSI Rome) and Prime Contractor is Rheinmetall Italia spa. MAGIA is an altimetry, gravimetric and geochemical mission consisting of a main Orbiter in polar orbit, which will release a Sub-satellite at the end of the mission. The scientific goals have been identified in order to avoid overlaps with currently planned, ongoing, or just concluded orbiter or impactor missions:

- study of the mineralogical composition of the Moon by means of a visible/near infrared (VIS/NIR) imaging spectrometer;

<sup>6</sup> Lunar Reconnaissance Orbiter

<sup>7</sup> Lunar Crater Observation and Sensing Satellite

- characterization of the Moon polar regions by means of concurrent observations with different instruments, (imaging experiment, altimeter and thermal);
- characterization of the lunar Gravity field with a two-satellite tracking similar to GRACE, with a main Orbiter and a small Sub-satellite;
- characterization of the lunar radiation environment by means of a particle radiation monitor;
- characterization of the lunar exosphere;
- fundamental physics test of gravity;
- absolute positioning metrology measurements;
- precursor technological test for 2<sup>nd</sup> generation LLR.

MAGIA is designed to reach its goals by exploiting for the Orbiter a new satellite concept, under development by Rheinmetall (derived from the MIOSAT<sup>8</sup> platform). The payload module will use instruments in an advanced development phase for other important planetary missions (BepiColombo, JUNO, Chandrayaan-1), like the Italian Spring Accelerometer (ISA, to be deployed on BepiColombo). This approach will make available innovative instruments of high technological content and a relatively moderate cost. The detailed science program, mission timeline and orbit evolution is described in detail elsewhere [28]. This work will exploit passive, maintenance-free laser retroreflectors and an atomic clock on the Orbiter.

With MAGIA we propose to perform the following experiments in the Earth-Moon system:

- VESPUCCI (Vega or Soyuz Payload for Unified Clock vs. Ccr Investigation): significant improvement of the measurement of the gravitational redshift in the trans-lunar flight and in Moon orbits. This will be illustrated in section 6.
- MoonLIGHT-P (Moon Laser Instrumentation for General relativity High-accuracy Test-Precursor): a technological test of the payload for 2<sup>nd</sup> generation LLR.
- Selenocenter: independent measurement of the position of the Moon center of mass with respect to the ITRF ([30], [31], [32]), until now performed using the Apollo and Lunokhod retroreflectors. MapRef: grid of absolute ITRF positions of MAGIA's lunar altimetry, gravity and geochemical maps, to be taken wherever the Orbiter can be tracked by LLR.

The retroreflectors will be tracked by the ILRS ([33], [34], [35]) with SLR and LLR. If MAGIA will be approved, the performance of the two retroreflector payloads will be characterized at the dedicated "Satellite/lunar laser ranging Characterization Facility (SCF)" of INFN-LNF ([36], [37], [38]). For the atomic clock analysis we consider a clock stability in the range between  $10^{-13}$  and  $2 \times 10^{-14}$ . Here we summarize the results of the Phase A study of the VESPUCCI experiment only.

### 6.1 VESPUCCI: Improved Measurement of the Gravitational Redshift

The acronym of the VESPUCCI experiment is due to the indication given by ASI during the 2007 lunar studies, that the launch vehicle of the robotic lunar missions could be a modified VEGA or a SOYUZ rocket.

The measurement of the gravitational redshift (GRS) is an important test of the Local Position Invariance (LPI) of General Relativity (GR) and of any metric theory of gravity.

Current experimental status is shown in Figure 26. The most accurate GRS measurement in space,  $|\alpha| < 2 \times 10^{-4}$ , was performed in 1976 by the satellite Gravity Probe A (GP-A, [39]), which employed a space-borne hydrogen-maser clock, reached a maximum orbital height of 10,000 Km and took data for about two hours.

The trans-lunar flight of MAGIA and the period the orbiter will spend around the Moon (~7 months) offer the possibility to perform an experimental test of the gravitational redshift in the Earth-Moon system based on CCR-Array (CCR-A), CCR-Moonlight (CCR-M) and an onboard atomic clock with

<sup>8</sup> Optical Mission based on a Microsatellite

relative frequency stability of  $10^{-13}$  or less. Positions on the ground and space clocks will be referenced to the ITRF. MAGIA is suited to improve significantly the GP-A measurement for the following reasons:

- the high-precision ISA and radio science (RS) payloads which ensure that the systematic error due to the Doppler shift background will be kept under control;
- lots of data will be acquired in a region between the Earth and the Moon where the two gravity fields can be considered simple point-like potentials, thus greatly simplifying the physics analysis;
- MAGIA will navigate two gravity potential wells experiencing the highest possible variation of GRS in the Earth-Moon system;
- MAGIA positioning with respect to the ITRF is achieved with two complementary techniques:
  - a. SLR/LLR tracking by the ILRS, which includes the Space Geodesy Center of ASI in Matera, Italy (ASI-CGS), providing very accurate and absolute distance determination with respect to the ITRF.
  - b. Mission radio telemetry from the ASI-CGS (and possibly, other stations).

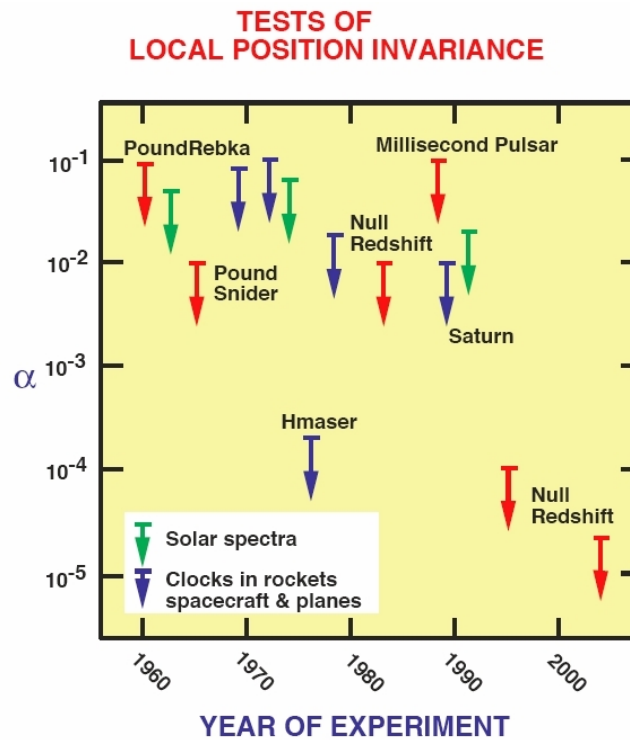


Figure 26: From Will (2006) [11]: “selected test of local position invariance via gravitational redshift experiments, showing bounds on  $\alpha$ , which measures degree of deviation of redshift from the formula  $\Delta v/v=(1+\alpha)\Delta U(r)/c^2$ . In null redshift experiments, the bound is on the difference between different kinds of clocks”.

Our goal is to improve the best direct limit by GP-A,  $|\alpha| < 2 \times 10^{-4}$ , with a clock of relative frequency stability of  $10^{-13}$  or less and Precise Orbit Determination (POD) with an absolute accuracy with the respect to ITRF of 10 m or less by means of radio tracking and SLR/LLR tracking of CCR-A and CCR-M. For the clock analysis we will consider a clock stability in the range between  $10^{-13}$  and  $2 \times 10^{-14}$ . Currently, our baseline clock is the RAFS (Rubidium Atomic clock Frequency Standard) and the target stability that we want to reach is  $5 \times 10^{-14}$  (but  $2 \times 10^{-14}$  seems achievable with the characterization described below). These clocks are manufactured for example by PerkinElmer (US),

are deployed on GPS-II<sup>9</sup> and will be deployed on GALILEO. Choice of a beyond-the-baseline clock may be possible depending on the level of funding and decisions to be taken at later mission phases. SLR provides station-to-satellite distance (single range) measurements with cm accuracy or less. For well-established orbits (like for LAGEOS) this amounts to a slightly larger accuracy on the absolute orbital trajectory (1-2 cm); but the less the SLR coverage of the orbit, the worse the absolute ITRF positioning. For a trans-lunar flight of about 1 week we assume very conservatively a degradation of POD SLR accuracy of a factor 100 (up to a few meters), which is still good enough for our goal. Around the Moon MAGIA orbits will be fully visible from ILRS stations for extended periods twice per month (once for CCR-A and once for CCR-M), as shown by Figure 27; however, with respect to the trans-lunar flight the laser return will decrease as  $1/(\text{distance})^4$ .

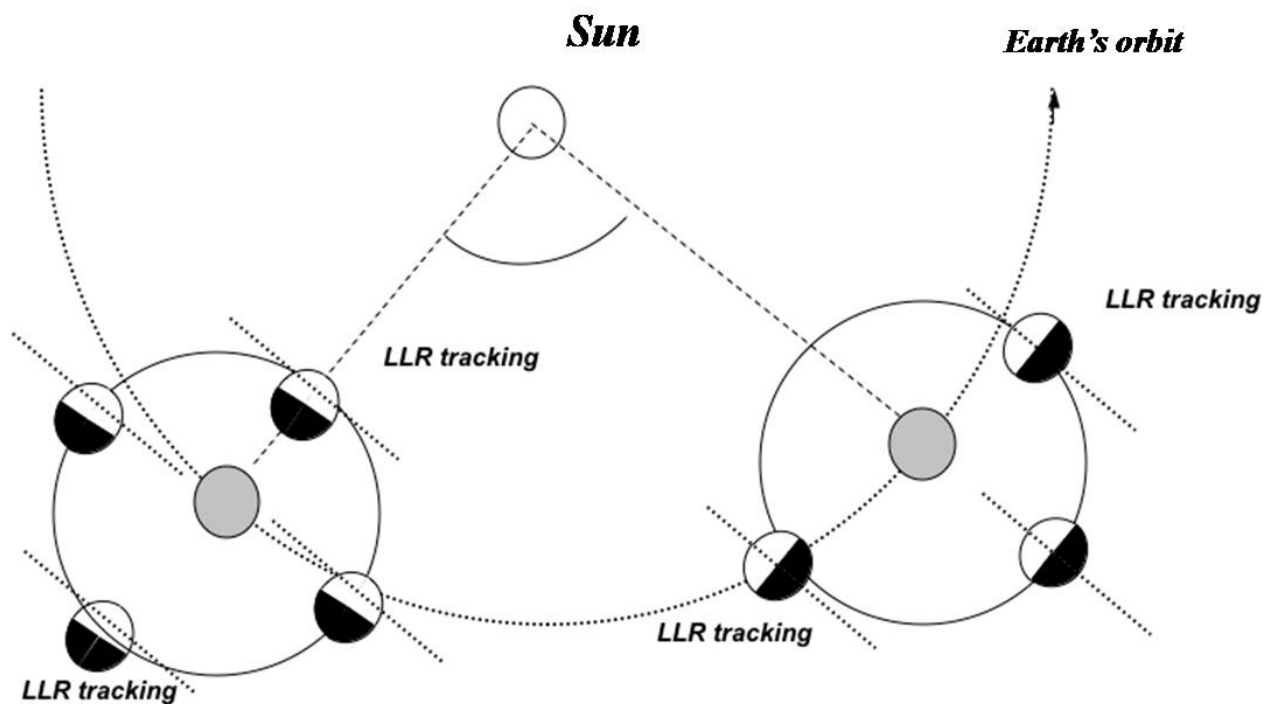


Figure 27: *LLR tracking of MAGIA with two different orbital configurations of the Moon, the Earth, the spacecraft and the sun illumination. CCR-A and CCR-M will be located on the different sides of the Orbiter in order to separate their laser returns to ground.*

MAGIA gives the unique opportunity to measure a varying GRS across the two potential wells of the Earth-Moon system. As shown in Figure 28, GRS will increase away from the Earth and slightly decrease near the Moon, up to the nominal MAGIA altitude of 100 Km over the Moon surface.

<sup>9</sup> Global Positioning System

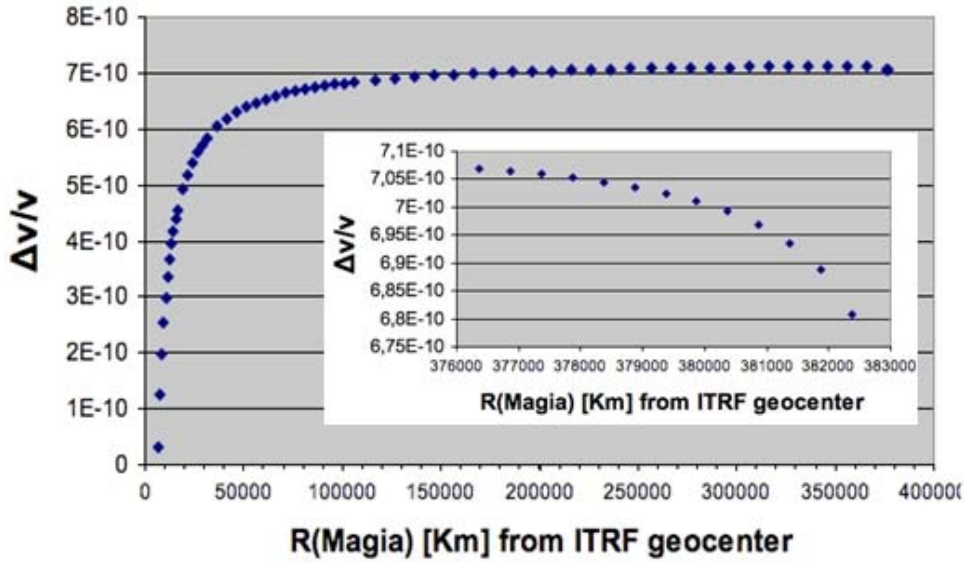


Figure 28: *GRS variation versus MAGIA distance from the geocenter, assuming point-like potentials. The inset shows a blow-out of the end point of the curve very near the Moon.*

Past experiments on airplanes [40] and spacecrafts [39] showed that variations of the GRS frequency shift ( $\Delta v$ ) with position,  $r$ , in the potential field ( $\Delta U(r)$ ) increase the statistical significance of test, as opposed to measuring a single GRS value at a single value of position  $r$ . They also showed that a detailed analysis is required to subtract Doppler shifts due to plane or spacecraft motion, and that tracking data are needed to determine the payload's location and the velocity (to evaluate the potential difference  $\Delta U$  and the special relativistic time dilation; see [32], [11]). Therefore, for MAGIA, the variation of  $\Delta v$  with distance (basically the maximum possible in the Earth-Moon system) will make our GRS measurement largely insensitive to systematic errors on the absolute frequency accuracy of the clock. For GR ( $\alpha = 0$ ) the  $\Delta v$  of MAGIA will be:

$$\Delta v = v_{MAGIA} - v_{Earth} = v_{offset} + \Delta U(r)/c^2 - v_{Earth}$$

where:

- $v_{offset}$  is the systematic error on the value of the RAFS absolute frequency. We will measure the absolute frequency accuracy with respect to a H-maser, to determine the residual sensitivity to  $v_{offset}$  which we think it will have a negligible effect for our goals.
- $v_{Earth}$  is the frequency of the reference H-maser(s) on Earth;
- $\Delta U(r_{MAGIA}) = GM(1/r_{MAGIA} - 1/r_{Earth})$  for point-like potentials. Our measurement will be sensitive only to this frequency variation with distance. Therefore, from the clock operation point of view, we only need to control its stability, that is, drift vs. time and its Allan variance vs time with the measured drift removed. This is an advantage that MAGIA has with respect to any GRS measurement attempted with nearly circular orbits, for which a single number,  $v_{offset}$ , has to be measured, instead of a frequency smoothly varying with distance (at least for GR).

GRS will be measured during the trans-lunar flight, with the satellite altitude controlled to make CCR-A array visible from the Earth, and in Moon orbits. Measuring the GRS in the Earth potential allows for a faster data analysis because the geo-potential is known much better than its lunar counterpart. Measuring the GRS around the Moon will require the completion of MAGIA gravimetric measurements.

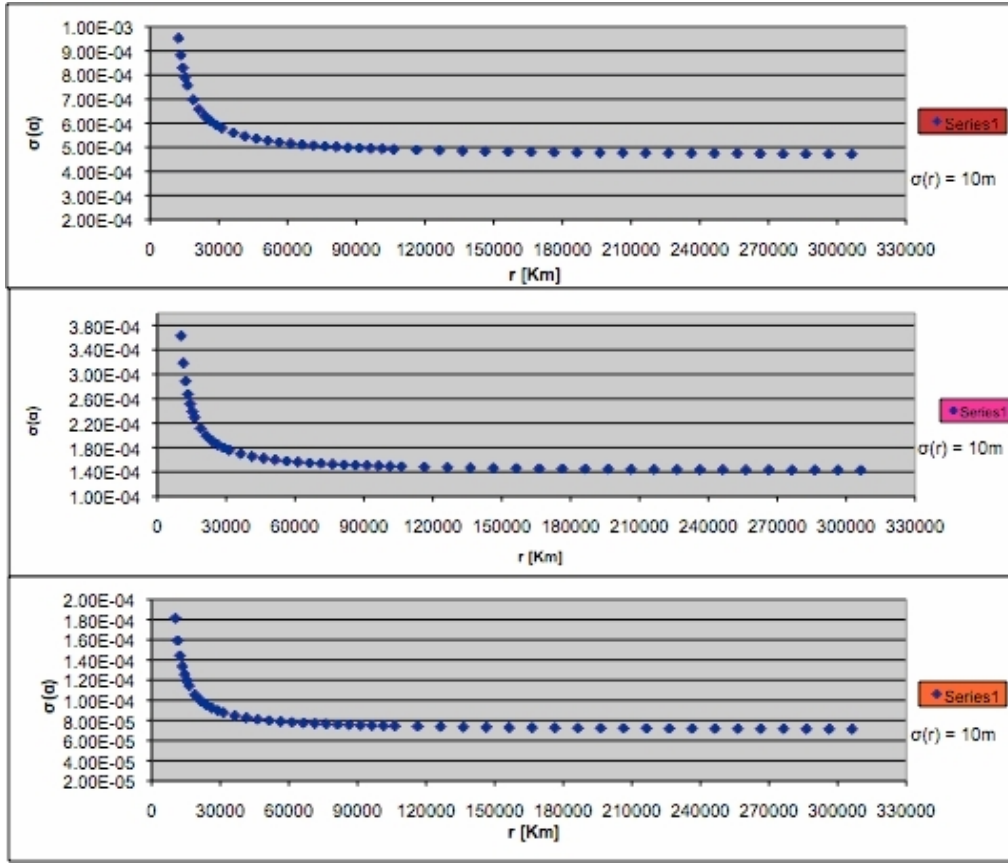


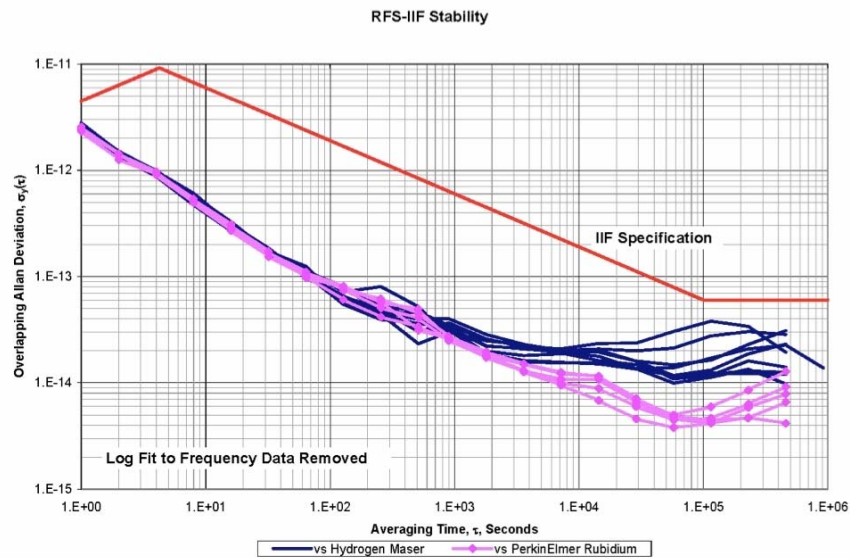
Figure 29: *Expected statistical error on the GRS test vs. distance from the ITRS geocenter.*

Finally, Figure 29 shows the expected statistical error on  $\alpha$  for single GRS measurements as a function of  $r_{\text{MAGIA}}$ , for a POD accuracy of 10 m and for three different clock accuracies of  $3.3 \times 10^{-13}$ ,  $10^{-13}$  and  $5 \times 10^{-14}$ . Assuming that the future measurement will agree with GR (e.g., it will yield a central value  $\alpha = 0$ ) we can take a weighted average of all measurement errors plotted in Figure 29, to get the following one standard deviation limits (at 68% CL, statistical uncertainty only):

1.  $|\alpha| < 8 \times 10^{-5}$  for a clock accuracy of  $3.3 \times 10^{-13}$ , a factor 2.5 improvement over GP-A.
2.  $|\alpha| < 2 \times 10^{-5}$  for a clock accuracy of  $10^{-13}$ , a factor 10 improvement over GP-A.
3.  $|\alpha| < 1 \times 10^{-5}$  for a clock accuracy of  $5 \times 10^{-14}$ , a factor 20 improvement over GP-A.

The above estimates are for  $r_{\text{MAGIA}} < 310,000$  Km. Using data up to 370,000 Km, the improvement will be larger. Note that Figure 30 shows that after 1 hr the stability of a calibrated RAFS is  $< 2 \times 10^{-14}$ , which corresponds to a GRS test improvement of a factor 50. The GRS measurement in Moon orbits will be done once the MAGIA lunar gravity potential will be ready. Then it will be combined with the Earth/trans-lunar flight GRS and it will give a further improvement of the test, up to an overall factor 100 of improvement over GP-A. Note that, if the MAGIA flight will be longer than 1 week (as it is foreseen in some alternative, beyond-the-baseline mission scenarios, where solar electric propulsion could be used for the transfer to the Moon), then the improvement will be significantly larger.

Finally, assuming GR is valid ( $\alpha = 0$ ), the measurement of the Moon GRS will also be an a posteriori high-level validation of the MAGIA gravity model.



2008 IEEE International Frequency Control Symposium – Honolulu Hawaii

Figure 30: Courtesy of PerkinElmer: RFS Allan variance measured with respect to a H-maser, with the measured drift removed, for a period of about 6 days.

The Phase A study was concluded in December 2008 with the final review and the full MAGIA Proposal was submitted to ASI. The MAGIA collaboration is now awaiting the decision of the new ASI management and the new National Space Plan. In the meantime, the work of the INFN-LNF group on the development of the MoonLIGHT-P prototype continued in 2009 in the framework of the ILN Core Instrument Working Group and with an *R&D experiment* approved by INFN for the period 2010-2012, called MoonLIGHT-ILN.

## 7. PLANETARY EPHEMERIS PROGRAM (PEP)

In the previous sections we have discussed how LLR measurements can be improved. Now we show selected aspects of LLR data analysis in progress, without, however, proving any new or final result.

In order to analyze LLR data we are using the Planetary Ephemeris Program (PEP) software [41], developed by the Center for Astrophysics (CfA), by I. Shapiro et al. starting from 1970s. PEP was designed not only to generate ephemerides of the Planets and Moon, but also to compare models with observations. One of the early uses of this software was the first measurement of the geodetic precession of the Moon [42]. There are a diverse set of observations that PEP can handle, but here we care primarily about LLR observations. In particular, the software is able to calculate the residuals of the distances between observed LLR data and computed data, derived from expectations of GR and of terrestrial and lunar Geodesy. We have performed a very preliminary analysis of LLR data from three stations: McDonald Observatory in Texas (USA), Grasse in France and APOLLO in New Mexico (USA). The latter station provides the best quality data since 2006. On March 25, 2010, the Matera Laser Ranging Observatory in Italy (MLRO, led by G. Bianco) recorded LLR echos from the array of Apollo 15.

The histograms in Figure 31 (lunar returns and fiducial/calibration returns) show photon-by-photon data and are used to form a single LLR “normal point” of the Apollo 15 array taken by the

APOLLO station (led by T. W. Murphy) on November 19, 2007. A normal point contains several information e.g. date of observation, atmospheric conditions, as well as time of flight, data quality and CCR arrays. The APOLLO instrumental accuracy (in terms of laser, detector, timing electronics, etc) shown by the fiducial returns in Figure 31 is a root mean square contribution of 120 ps (18 mm)

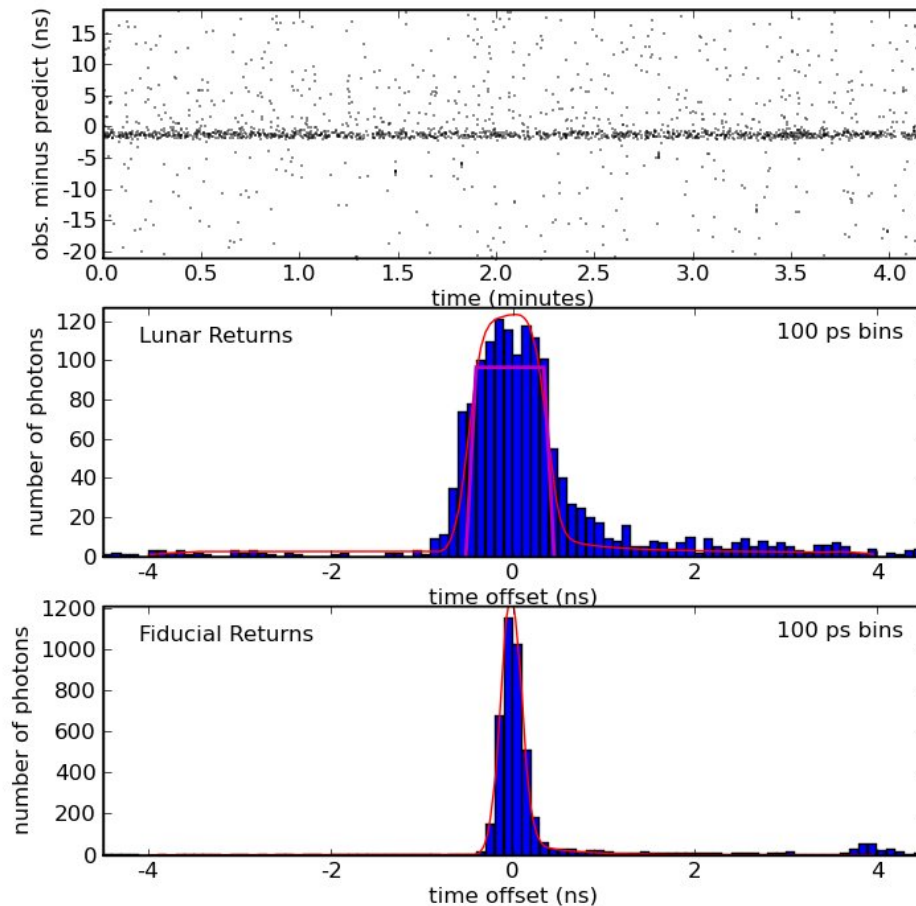


Figure 31: *Example run of Apollo 15. In the plot, the top panel shows a 40 ns window of observed round trip time minus the predicted range. Background noise and detector dark current appear as scattered dots, while the lunar return is in the middle. The middle panel shows a histogram of the lunar returns, while the bottom panel shows the local "fiducial" CCR return, fitted by the red Gaussian. The Lunar return is additionally spread by the tilted reflector array modeled by the superimposed magenta trapezoidal shape; [43].*

From a comparison between the middle and the last plot we can see how the tilt in the arrays affects the accuracy of the ranging measurements. The model parameter estimates are refined by minimizing the residual differences, in a weighted least-squares sense, between observations (O) and model predictions (C, stands for 'Computation'), O-C. "Observed" is round-trip time of flight. "Computed" is modeled by the PEP software.

We study the internal quality of the experimental data and the PEP modeling of the lunar librations and Earth rotations. Within a single day, differences between (O-C)'s (as well as O's and C'

independently) should have a very small variation, mainly sensitive to the internal experimental accuracy and to relative Earth-Moon rotations. So we consider the quantity  $|\max(\text{O-C}) - \min(\text{O-C})|$  for days where multiple normal point measurements were recorded for Apollo 11, 14 and 15 in the same day.

Figure 32 shows the  $|\max(\text{O-C}) - \min(\text{O-C})|$  of all Apollo LRAs, using normal points from the APOLLO station data set taken from 2006 to 2009.

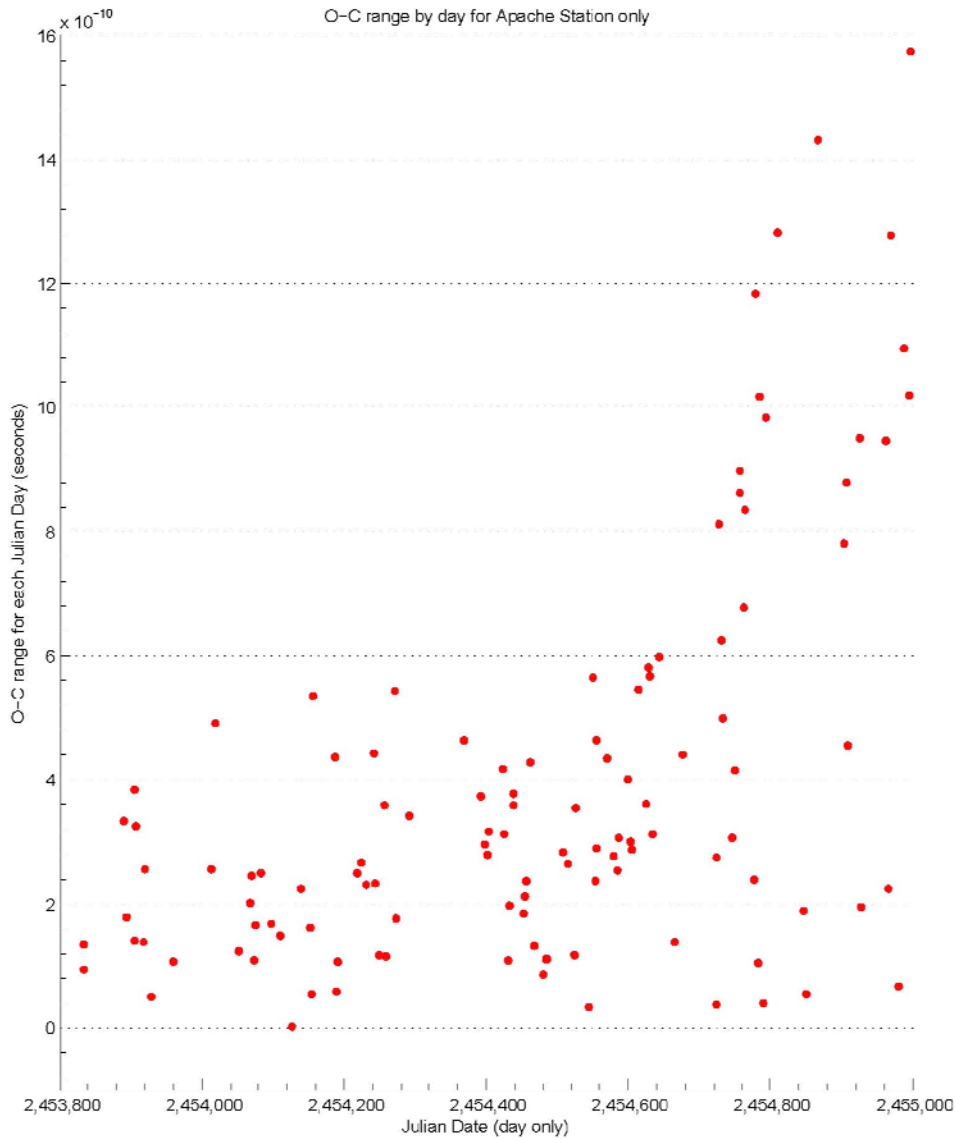


Figure 32: APOLLO  $|\max(\text{O-C}) - \min(\text{O-C})|$  range data pre-processed by PEP and then analyzed as explained in the text.

The PEP software has enabled constraints on departures from standard physics. For example, it has been used to place limits on the PPN parameters  $\beta$  and  $\gamma$ , geodetic precession and the variation of the gravitational constant,  $\dot{G}/G$  (see [44], [45], [46]).

The INFN-LNF group is working on the spacetime torsion model reported in section 2. The spacetime torsion equation of motions could be included in PEP software and constrained with

newest APOLLO data. Note that constraints on spacetime torsion parameters shown in Figure 7 are calculated using old LLR and MRR data (see [13] and references therein).

## 8. CONCLUSION

The Lunar Laser Ranging LLR technique provides very precise, metrologically absolute and cost effective measurements in the Sun-Earth-Moon system laboratory. LLR has given important and precise tests of several predictions of General Relativity (Equivalence Principle, geodetic precession, parameterized post-Newtonian parameters  $\gamma$  and  $\beta$ , the constancy of the gravitational constant  $G$ ), as well as a constraint on a new theory of spacetime torsion.

The US-Italy R&D effort carried out since 2006 demonstrated that the current, dominant source of uncertainty in the Moon orbit accuracy (few centimeters) can be completely removed by deploying large ‘solo’ CCRs: the MoonLIGHT/LLRRA21 payloads. We will continue further thermal-vacuum-optical testing of the payload at the SCF. Specific payload design adaptations have been considered for deployment on a lander, a rover, and an orbiter (like MAGIA). We also performed a first structural analysis to meet launch requirements. Investigations of lunar regolith drilling capabilities are in progress.

The modern vision of an international, geopolitically-free physical/geophysical network on the lunar surface is embodied by the ILN. In the ILN concept, there are several nodes, from a minimum of 6, that would include at least four “core” instruments: seismometer, heat flow probe, laser retroreflector, electromagnetic sounder. Individual nodes could and likely would carry additional, unique experiments to study local or global lunar science. Nine countries have formed the ILN partnership (<http://iln.arc.nasa.gov/>) and set up four working groups, which study: 1) Core Instrument; 2) Communications; 3) Site selection; 4) Enabling technologies. The MoonLIGHT/LLRRA21 payload concept is indicated as the choice of interest in the final report of the ILN Core Instruments working group [48] The ILN communications are discussed in another final report [49]. Concerning the choice of new laser retroreflector sites, we would like to increase as much as possible the north-south and east-west spread of locations on the near side of the Moon. As shown by Figure 4, any new retroreflector in the southern hemisphere would be most useful, since there is none south of -4 degrees.

Finally, thanks to the new, high-performance LLR station, APOLLO, and the availability of the PEP software package, the LLR gravitational science, initiated more than 40 years ago with Apollo and Luna missions, will have further fruitful development with the new wave of lunar surface research and exploration.

## 9. ACKNOWLEDGMENTS

We wish to acknowledge the support of the INFN for the construction and operation of the SCF with the ETRUSCO<sup>10</sup> experiment [24], for the development of the MoonLIGHT/LLRRA21 payload with the dedicated MoonLIGHT/LLRRA21 experiment (all in the framework of the “Commissione Scientifica Nazionale V”, CSNV). We also acknowledge the University of Maryland via the NASA “Lunar Science Sortie Opportunities” program<sup>11</sup> to investigate Lunar Science for the NASA Manned Lunar Surface Science and the LUNAR consortium (<http://lunar.colorado.edu>),

---

<sup>10</sup> Extra Terrestrial Ranging to Unified Satellite Constellations.

<sup>11</sup> Contract NNX07AV62G.

headquartered at the University of Colorado, which is funded by the NASA Lunar Science Institute<sup>12</sup> to investigate concepts for astrophysical observatories on the Moon. We also wish to thank ASI for the support during the 2007 lunar studies<sup>13</sup> and the 2008 Phase A study for the proposed MAGIA mission<sup>14</sup>.

## 10. REFERENCES

- [1] Bender P. L., et al, "The Lunar Laser Ranging Experiment", *Science*, Volume 182, Issue 4109, pp. 229-238, 1973.
- [2] Dell'Agnello S., Currie, G. C., Delle Monache, G. O., Cantone C., Garattini M., Martini M., Intaglietta N., Lops C., March R., Tauraso R., Bellettini G., Maiello M., Berardi S., Porcelli L.; "Next Generation Lunar Laser Ranging and its GNSS Applications"; IEEE Aerospace Conference, Big Sky (MT), USA, March 2010 - Conference Proceeding.
- [3] Williams J. G., Turyshev S. G., Boggs D. H., Ratcliff J.T., "Lunar Laser Ranging Science: Gravitational Physics and Lunar Interior and Geodesy", 35th COSPAR Scientific Assembly, July 18-24, 2004.
- [4] Williams J. G., Boggs D. H., Ratcliff J. T., "A larger lunar core?", 40th Lunar and Planetary Science Conference, March 23-27, 2009.
- [5] Williams J. G., Turyshev S. G., Boggs D. H., "Lunar Laser Ranging Test of the Equivalence Principle with the Earth and Moon", *Int. J. Mod. Phys. D*, Volume 18, 1129-1175, 2009.
- [6] Rambaux N., Williams J. G., Boggs D. H., "A Dynamically Active Moon-Lunar Free Librations and Excitation Mechanisms", 39th Lunar and Planetary Science Conference, March 10-14, 2008.
- [7] Williams J. G., Boggs D. H., Ratcliff J. T., "Lunar Tides, Fluid Core and Core/Mantle Boundary", 39th Lunar and Planetary Science Conference, March 10-14, 2008.
- [8] Murphy T., Battat J., et al., "The Apache Point Observatory Lunar Laser-Ranging Operation (APOLLO): two years of Millimeter-Precision Measurements of the Earth-Moon Range", *PASP* 121, 29 (2009).
- [9] Riess A. G., Filippenko A. V., Challis P., Clocchiatti A., Diercks A., Garnavich P. M., Gilliland R. L., Hogan C. J., Jha S., Kirshner R. P., Leibundgut B., Phillips M. M., Reiss D., Schmidt B. P., Schommer R. A., Smith R. C., Spyromilio J., Stubbs C., Suntzeff N. B., Tonry J., "Observational Evidence from Supernovae for an Accelerating Universe and a Cosmological Constant", *The Astronomical Journal*, 116:1009-1038, 1998 September.
- [10] Kolb E. W., Matarrese S., Riotto A., "On cosmic acceleration without dark energy", *New J. Phys.* 8 (2006) 322.
- [11] Will, C. M., "The Confrontation between General Relativity and Experiment", *Living Rev. Relativity*, 9, (2006), 3.
- [12] Bertotti B., Iess L., Tortora P., "A test of general relativity using radio links with the Cassini spacecraft", *Nature* 425, 374-376 (25 September 2003).
- [13] March R., Bellettini G., Tauraso R., Dell'Agnello S., "Constraining spacetime torsion with the Moon and Mercury", arXiv:1101.2789v1 [gr-qc] 14 Jan 2011.
- [14] March R., Bellettini G., Tauraso R., Dell'Agnello S., "Constraining spacetime torsion with LAGEOS", arXiv:1101.2791v1 [gr-qc] 14 Jan 2011
- [15] Mao Y., Tegmark M., Guth A. H., and Cabi S., "Constraining torsion with Gravity Probe B", *Phys. Rev. D* 76, 104029 (2007).

---

<sup>12</sup> via Cooperative Agreement NNA09DB30A

<sup>13</sup> Contract I/032/06/04

<sup>14</sup> ASI-INAF/MAGIA n. 20080508-1

- [16] Flanagan E.F., Rosenthal E., Phys. Rev. D 75, 124016 (2007).
- [17] Murphy T. W., Adelberger E. G., Strasburg J. D., Stubbs C. W., Nordtvedt K., “Testing Gravity via Next Generation Lunar Laser-Ranging”, Nuclear Physics B Proceedings Supplements, Volume 134 (2004), 155-162.
- [18] Nordtvedt K., “Testing the Equivalence Principle with laser ranging to the Moon”, J. Adv. Space Res., Volume 32, Issue 7, 1311-1320, 2003.
- [19] Williams J. G., Turyshev S. G., Boggs D. H., “Progress in Lunar Laser Ranging Tests of Relativistic Gravity”, Phys. Rev. Lett. 93, 261101 (2004).
- [20] Nordtvedt K., “Lunar Laser Ranging: a comprehensive probe of post-Newtonian gravity”, Gravitation: from the Hubble length to the Planck length, edited by Ciufolini I., Coccia E., Gorini V., Peron R., Vittorio N., ISBN 075030948, published by Institute of Physics Publishing, the Institute of Physics, London, 2005, p.97.
- [21] Nordtvedt K., and Vokrouhlicky D. (1997), "Recent Progress in Analytical Modeling of the Relativistic Effects in the Lunar Motion", in: "Dynamics and Astronomy of the Natural and Artificial Celestial Bodies", eds: I.M. Wytrzyszczak, J.H. Lieske and R.A. Feldman (Kluwer Academic Publishers, Dordrecht), p.205.
- [22] Courtesy of Coy J., Fischbach E., Hellings R., Talmadge C. and Standish E. M. (2003).
- [23] Merkwowitz S., Aaron E., Ashby N., Carrier D., Currie D., Degnan J. J., Dell’Agnello S., Delle Monache G., McGarry J., Murphy T. W., Nordtvedt K., Reasenberg R. D., Shapiro I. I., Turyshev S. G., Williams J. G., Zagwodzk T., “The Moon as a Test Body for General Relativity”, white paper submitted to Planetary Science Decadal Survey, September 2009.
- [24] Dell’Agnello S., Delle Monache G. O., Currie D. G., Vittori R., Cantone C., Garattini M., Boni A., Martini M., Lops C., Intaglietta N., Tauraso R., Arnold D. A., Pearlman M. R., Bianco G., Zerbini S., Maiello M., Berardi S., Porcelli L., C. O. Alley, J. F. McGarry, C. Sciarretta, V. Luceri, T. W. Zagwodzki, “Creation of the New Industry-Standard Space Test of Laser Retroreflectors for the GNSS and LAGEOS”; J. Adv. Space Res. (2010), DOI: 10.1016/j.asr.2010.10.022.
- [25] Boni A., Cantone C., Dell’Agnello S., Delle Monache G. O., Garattini M., Intaglietta N., Lops C., Martini M., Porcelli L., “Optical far field diffraction pattern test of laser retroreflectors for space applications in air and isothermal conditions at INFN-LNF”, INFN-LNF Report LNF-08/26(IR), 2008.
- [26] Dell’Agnello S., Currie D. G., Delle Monache G. O., Lops C., Martini, M., “LLRRA21/MoonLIGHT: a 2<sup>nd</sup> Generation Lunar Laser Ranging Array for Precision Gravity Tests and Lunar Science Measurements”, Global Lunar Conference (GLUC) 2010 – Beijing, China 31 May-3 June 2010 - Conference Proceeding.
- [27] Currie D. G., Dell’Agnello S., Delle Monache G. O., “A Lunar Laser Ranging Retroreflector Array for the 21st Century” J. Acta Astronautica (2010), DOI: 10.1016/j.actaastro.2010.09.001.
- [28] Dell’Agnello S., Lops C., Delle Monache G. O., Currie D. G., Martini M., Vittori R., Coradini A., Dionisio C., Garattini M., Boni A., Cantone C., March R., Bellettini G., Tauraso R., Maiello M., Porcelli L., Berardi S., Intaglietta N., “Fundamental physics and absolute positionin metrology with the MAGIA lunar orbiter” Exp. Astron., July 2010, DOI: 10.1007/s10686-010-9195-0.
- [29] Di Salvo A., Agostara C., Coradini A., Dionisio C., Orosei R., Falvella M. C., Tuninetti C., “MAGIA, the Italian mission for geodesy, geophysics and geochemistry of the Moon”, Global Lunar Conference (GLUC) 2010 – Beijing, China 31 May-3 June 2010 - Conference Talk
- [30] <http://itrf.ensg.ign.fr/>

- [31] Altamimi Z., Collilieux X., Legrand J., et al.: "ITRF2005: a new release of the International Terrestrial Reference Frame based on time series of station positions and Earth orientation parameters" *J. Geophys. Res.*, 112(B9), B09401 (2007).
- [32] Geodesist's Handbook: Bulletin Geodesique, 66. Springer, Berlin (1992).
- [33] Pearlman M. R., Degnan J. J., and Bosworth J.M., "The International Laser Ranging Service", *J. Adv. Space Res.*, Vol. 30, No. 2, pp. 135-143, July 2002, DOI: 10.1016/S0273-1177(02)00277-6.
- [34] <http://ilrs.gsfc.nasa.gov/>.
- [35] Pearlman M.R., Degnan J.J., Bosworth, J.M., "The International Laser Ranging Service", *Advances in Space Research*, Vol. 30, No. 2, pp. 135-143, July 2002, DOI:10.1016/S0273-1177(02)00277-6.
- [36] Bosco, A. et al, "Probing Gravity in NEOs with High-Accuracy Laser-Ranged Test Masses", *International Journal of Modern Physics D*, Vol. 16, No. 12A (2007), 2271-2285.
- [37] Dell'Agnello, S. et al, "Creation of the Industry-standard Space Test of Laser Retroreflectors for GNSS, Fundamental Physics and Space Geodesy: the "SCF-Test"", *Proceedings of the 1<sup>6</sup><sup>th</sup> International Workshop on Laser Ranging (2008)*, Poznan, Poland.
- [38] Dell'Agnello, S. et al, "A Lunar Laser Ranging Array for NASA's Manned Landings, the International Lunar Network and the Proposed ASI Lunar Mission MAGIA", *Proceedings of the "16<sup>th</sup> International Workshop on Laser Ranging" (2008)*, Poznan, Poland.
- [39] Vessot R. F. C., et al., "Test of Relativistic Gravitation with a Space borne Hydrogen Maser" *Phys. Rev. Lett.* 45, 2081-2084 (1980).
- [40] Alley C. O., et al in "Experimental Gravitation", *Proceedings of the Conference at Pavia, Italy (September 1976)*, edited by B. Bertotti (Academic, New York, 1977).
- [41] Urschl C., Beutler G., Gurtner W., Hugentobler U., Schaer S., "Contribution of SLR tracking data to GNSS orbit determination", *J. Adv. Space Research*, 39(10), 1515-1523, 2007.
- [42] Shapiro I. I., Reasenberg R. D., Chandler J. F., "Measurement of the de Sitter Precession of the Moon: A Relativistic Three-Body Effect", *Phys. Rev. Lett.* 61, 2643-2646 (1988).
- [43] <http://www.physics.ucsd.edu/~tmurphy/apollo/highlights.html>
- [44] Battat J. B. R., Stubbs C. W., Chandler J. F., "Solar system constraints on the Dvali-Gabadadze-Porrati braneworld theory of gravity", *Phys. Rev. D*, 78, 022003, 2008.
- [45] Reasenberg R. D., Shapiro I. I., MacNeil P. E., Goldstein R. B., Breidenthal J. C., Brenkle J. P., Cain D. L., Kaufman T. M., Komarek T. A., Zygielbaum A. I., *Astrophysical. Journal Letters* 234, L219 (1979).
- [46] Chandler J. F., Reasenberg R. D., Shapiro I. I., in *Proceedings of the Seventh Marcel Grossman Meeting on recent developments in theoretical and experimental general relativity, gravitation, and relativistic field theories*, edited by Jantzen R. T., Mac Keiser G., Ruffini R. (1996), p. 1501.
- [47] Dell'Agnello S., Delle Monache G.O., Currie D.G., Martini M., Lops C., Garattini M., March R., Bellettini G., Tauraso R., Battat J.B., Bianco G., Murphy T.W., Coradini A., Chandler J.F., Boni A., Cantone C., Maiello M., Porcelli L., Berardi S., Intaglietta N., Patrizi G, "The Moon as a test body for General Relativity and new Gravitational Theories", poster to the conference EPSC2010, 19 - 24 September 2010, Rome, Italy.
- [48] <http://iln.arc.nasa.gov/sites/iln.arc.nasa.gov/files/WorkingGroups/WorkingGroups2.pdf>
- [49] [http://iln.arc.nasa.gov/sites/iln.arc.nasa.gov/files/ILN\\_Core\\_Instruments\\_WG\\_v6.pdf](http://iln.arc.nasa.gov/sites/iln.arc.nasa.gov/files/ILN_Core_Instruments_WG_v6.pdf)